ADDIS ABABA UNIVERSITY

ADDIS ABABA INSTITUTE OF TECHNOLOGY

SCHOOL OF CIVIL AND ENVIRONMENTAL ENGINEERING

Structural Response Evaluation of Concrete Sleeper under Increasing Train Speed and Axle Load

---

A Thesis in Civil Engineering

by

Tibebu Paulos

Submitted in Partial Fulfilment of the Requirements for the Degree of Master of Science

October 2016

DECLARATION

I hereby certify that the research work titled ‘Structural Response Evaluation of Concrete Sleeper under Increasing Train Speed and Axle Load’ is my own work. The work has not been presented elsewhere for assessment. Where material has been used from other sources it has been properly acknowledged.

Tibebu Paulos

ABSTRACT

Nowadays the railway tracks are subjected to high train speed and freight tonnage which in turn cause deterioration to track components and affect the geometry and service life of the track.

The type of track loading and its quantity combined with varying traffic conditions have a great effect on the structural behaviour of sleepers. Hence the need for studying the sleepers' structural response under different loading conditions such as increasing train speed and axle load is of great significance.

To study the effects of increase in speed and axle load on the structural response of prestressed concrete sleeper, a three-dimensional ballast track and a separate concrete sleeper with a detailed feature are modelled by using commercial finite element package, ANSYS.

Speed is considered at four different rates which are 80, 120, 160 and 200 km/h and axle load at 23, 25, 27 and 29 ton. Since it is practical to improve track property before increasing load above its design limit, the existing track model (Model 1) is modified to obtain a track model with better rail profile and pad stiffness (Model 2) and the effect of track improvement on structural response of the sleeper is investigated.

Two types of ballast support conditions, which are mentioned in AREMA manual, are also considered to investigate the effect of difference in support condition. These support conditions are categorised as Case 1($L_{eff} \cong 2L/3$) and Case 2 ($L_{eff} = L$) for the purpose of this thesis. Both dynamic and static structural analyses are employed to get rail seat load from the track models and to analyse the response of prestressed concrete sleeper respectively.

The analysis results show that the increase in speed from 80 to 200 km/h which is 150% increment increases the bending stress and deflection in about 40.3% and increase in axle load from 23 ton to 29 ton which is about 26.1% increment increases the bending stress and deflection in about 26.1% with Model 1. With the same increment in speed and axle load, improving the track model (Model 2) reduced the percentage increment of bending stress and deflection by about 13.8% in the case of speed and 12.6% in the case of axle load.

This indicates the bending stress and deflection of the sleeper are affected slightly by the speed variation while axle load increment affects significantly.

Key words:- Concrete Sleeper, Train Speed, Axle Load, Ballast Pressure

ACKNOWLEDGMENTS

First of all I would like to thank the Almighty God for His love and help in all the situations of my life.

I would like to thank my advisor Mr. Mequanent Mulugeta for his invaluable guidance and supervision throughout this work.

I would also like to express my gratitude to Ethiopian Railways Corporation (ERC) for the sponsorship.

Finally, I'm so grateful to my beloved family and friends for being by my side as always.

TABLE OF CONTENTS

LIST OF TABLES

LIST OF FIGURES

Notation

E_c	Elastic moduli of a concrete
E_s	Elastic moduli of non-prestressed steel
E_P	Elastic moduli of prestressed steel
f_c	The compressive strength of concrete at 28 days
f_{ctk}	Concrete flexural tensile strength under static load at the age of 28 days
f_p	Ultimate strength of the prestressing steel
f_{ptk}	Characteristic strength for prestressed steel wire
L	Length of sleeper
L_{eff}	Effective length of sleeper
ρ_c	Density of concrete in kilogram per cubic meter
ρ_s	Density of tendon in kilogram per cubic meter
v_c	Poison's ratio of concrete
v_s	Poison's ratio of steel tendon

Acronyms

AREMA	American Railway Engineering and Maintenance-of-Way Association
CWR	Continuously Welded Rail
ERC	Ethiopian Railways Corporation
FEA	Finite Element Analysis
FEM	Finite Element Method
LRT	Light Rail Transit
RSL	Rail Seat Load

CHAPTER 1 INTRODUCTION

1.1 Background

The railway track system is an important part of the transportation infrastructure of a country and plays a significant role in sustaining a healthy economy. The annual investment of funds to construct and maintain a viable track system is enormous. The optimum use of these funds is a challenge which demands the best technology available. Unfortunately the pressure on a rail road to reduce operating costs usually result in cutting or eliminating investment in technology because it often does not generate a short term return on investment. [1]

Currently Ethiopia is constructing new railway tracks to fulfil the demand of transportation in the country for both passenger and freight. This construction covers both the LRT for Addis Ababa city and national railway networks. And under these constructions concrete sleepers are used as one of the main components of the track superstructure.

Sleepers are essentially beams that span across and tie together the two rails. They receive the load from the rail and distribute it over the supporting ballast at an acceptable ballast pressure level, hold the fastening system to maintain proper track gauge, restrain the lateral, longitudinal and vertical rail movement by anchorage of the superstructure in the ballast, and provide a cant to the rails to help develop proper rail-wheel contact by matching the inclination of the conical wheel shape. [2]

The sleeper and fastening deterioration depends on traffic and operational factors such as axle loads, speeds, accumulative tonnage and maintenance practices.

Concrete sleepers deterioration composes:-sleeper cracking, loosening of fastenings when support of the sleeper is inadequate and abrasion of the soffit due to excessive movement of sleepers or bad ballast conditions. A vital factor for the fastenings in track to function successfully is the condition of the sleepers. [2]

As described by [2] axle load and train speed are the two main factors controlling wheel/rail impact forces. Increasing the speed of trains has many effects on rail and track behaviour and degradation. Axle loads affect rail head wear, fatigue of the rail steel and plastic flow and shelling in the running surface between wheel and rail head. Greater

axle loads lead to increased wheel wear and higher bending stress in rails and sleepers, as well as higher bearing stress in ballast and subgrade.

This thesis focuses on studying the structural response of concrete sleepers under varying conditions of track loading such as increasing train speed and axle load. This will be done by modelling and analysing a typical ballast track and separate concrete sleeper by using FEM.

1.2 Statement of the Problem

In railways increasing demand for transportation of passengers and freight increased the need of higher speed and axle load. These conditions highly affect the service life of track components such as sleepers.

Though the effects of increasing speed and axle load are not the current problems of Ethiopian railway lines, in the future as the demand for transportation increases there will be a need to improve the train speed and increase axle load. These changes in turn cause deterioration to track components such as sleepers, affect the geometry and service life of the track. To ensure sufficient capacity of sleepers to support further increase in speed and axle load and to examine and improve current design practices their structural response under these conditions should be studied.

1.3 Objective

1.3.1 General objective

To study the effect of increasing train speed and axle load on structural response of concrete sleeper under different types of ballast support conditions by using Finite Element Analysis (FEA) method.

1.3.2 Specific objective

The specific objective of this research is

- to model and analyse the response (bending stress and deflection) of prestressed concrete sleeper under increasing train speed and axle load by using FEA method
- to study the effect of improving track property on the structural response of prestressed concrete sleeper under increasing train speed and axle load

- to study the effect of different ballast support conditions on the sleeper structural behaviour under increasing train speed and axle load
- to study the structural response of concrete sleepers currently being used in Ethiopian national railway lines in the case of higher speed and axle load than intended

1.4 Methodology

Technical papers, journals and publications which focus on the design, loading condition, failure mechanisms, etc. of prestressed concrete sleepers are reviewed.

Data needed for the research is collected from Ethiopian Railways Corporation (ERC), American Railway Engineering and Maintenance of Way Association (AREMA) manual, Chinese standard and other acknowledged publications.

Generally this research work undergoes in the following manner

- input parameters which are obtained from ERC, AREMA, Chinese standard, etc. are summarized for the modelling
- three dimensional ballast track is modelled in ANSYS commercial software package
- transient load is applied on the rail for dynamic analysis and the rail seat load is obtained for various speeds and axle loads from two different track models
- a separate three dimensional concrete sleeper with a detailed feature is modelled
- static structural analysis is employed to study the response (bending stress and deflection) of the sleeper

CHAPTER 2 LITERATURE REVIEW

2.1 Introduction

Rail track network forms an essential part of the transportation system of a country and plays a vital role in its economy. It is responsible for transporting freight and bulk commodities between major cities, ports and numerous mineral and agricultural industries, apart from carrying passengers in busy urban networks. In recent years, the continual competition with road, air and water transport in terms of speed, carrying capacity and cost have substantially increased the frequency and axle load of the trains with faster operational speeds. On one hand this implies continuous upgrading of track, and on the other, this imparts inevitable pressure for adopting innovative technology to minimize construction and maintenance costs. Hundreds of millions of dollars are spent each year for the construction and maintenance of rail tracks in many countries including USA, Canada, China, India and Australia. The efficient and optimum use of these funds is a challenging task which demands innovative and cutting edge technologies in railway engineering. [3]

The purpose of a railway track structure is to provide a stable, safe and efficient guided platform for the train wheels to run at various speeds with different axle loadings. To achieve these objectives, the vertical and lateral alignments of track must be maintained and each component of the structure must perform its desired functions satisfactorily under various axle loads, speeds, environmental and operational conditions. [3]

The track experiences vertical, horizontal and longitudinal forces. These forces influence the functions of the basic components in the track which in turn affect degradation and the failure process. The failure of each component has an effect on the function of other components in the track system. [2]

2.2 Track Structure and Components

The purpose of railway structure is to provide safe and economical train transportation. This requires the track to serve as a stable guideway with appropriate vertical and horizontal alignment. To achieve this role each component of the system must perform

its specific functions satisfactorily in response to the traffic loads and environmental factors imposed on the system.

The main components of ballasted track structures may be grouped into two main groups, superstructure and substructure. The superstructure consists of the rails, the fastening system and the sleepers (ties). The substructure consists of the ballast, the subballast and the subgrade. Thus the superstructure and substructure are separated by the sleeper-ballast interface. [1]

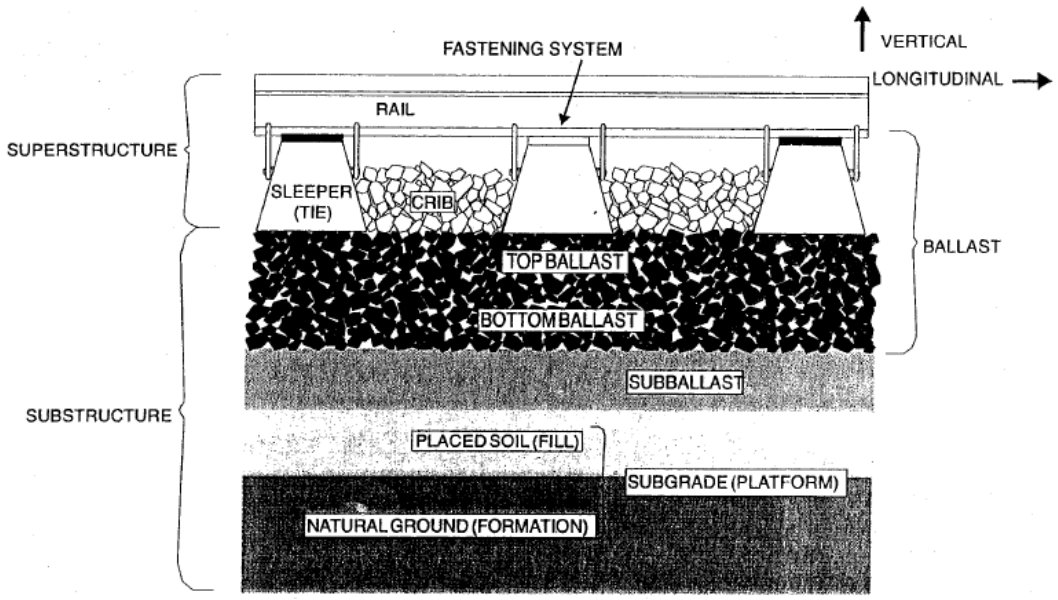

Figure 2-1 Track structure components [1]

Rail

Rails are the longitudinal steel members that directly guide the train wheels evenly and continuously. They must have sufficient stiffness to serve as beams which transfer the concentrated wheel loads to the spaced sleeper supports without excessive deflection between supports. The profile of the rail surface together with the wheel profile influences the guidance of the vehicles as they roll. Also rail and wheel surface defects can cause large dynamic loads which are detrimental to the track structure. [1]

Railpad

In a railway track with concrete sleepers, railpads are placed between the steel rails and the sleepers. The railpads protect the sleepers from wear and impact damage, and they provide electrical insulation of the rails. From a track dynamics point of view, the

railpads play an important role. They influence the overall track stiffness. When the track is loaded by the train, a soft railpad permits a larger deflection of the rails and the axle load from the train is distributed over more sleepers. [4]

Sleeper

Sleepers provide a resilient, even and flat platform for holding the rails, and form the basis of a rail fastening system. The rail-sleeper assembly maintains the designed rail gauge. Sleepers are laid on top of the compacted ballast layer a specific distance apart. During the passage of trains, the sleepers receive concentrated vertical, lateral and longitudinal forces from the rails, and these forces are distributed by the sleepers over a wider area to decrease the stress at the sleeper/ballast interface to an acceptable level.

Pre-stressed concrete sleepers are potentially more durable, stronger, heavier, and more rigid than their timber counterparts. A main advantage is that the geometry of the concrete sleepers can be easily modified to extend the support area beneath the rails. The extended support area decreases the ballast/sleeper contact stress, hence minimizing track settlement and particle breakage. [3]

Ballast, subballast and subgrade

Ballast is the select crushed granular material placed as the top layer of the substructure in which the sleepers are embedded.

Traditionally angular crushed hard stones and rocks uniformly graded free of dust and dirt and not prone to cementing action have been considered good ballast materials.[1]

Subballast is material chosen as a transition layer between the upper layer of large particle, good quality ballast and the lower layer of fine-graded subgrade. The subballast used in most new constructions is intended to prevent the mutual penetration of the subgrade and the ballast and to reduce frost penetration. Any sand or gravel materials may serve as subballast material as long as they meet necessary filtering requirements. [4]

Subgrade, or formation, is a surface of earth or rock levelled off to receive a foundation for the track bed. Sometimes an extra layer, a formation layer, is put on the earth so as to give the correct profile of the track bed. On this material the subballast and ballast layers rest.[2]

2.3 Dynamic property of track components

2.3.1 Rail

Bending vibration of a free rail mathematically modelled as there is no support along the rail; the rail is supported only at the boundaries.

The rail may be modelled either as an ordinary Euler- Bernoulli (E-B) beam or as a Rayleigh-Timoshenko (R-T) beam.[4]

Euler-Bernoulli (E-B) beam

In this theory, only the bending of the rail is taken into account, and in case of vibrations, only the mass inertia in translation of the beam is included.

The differential equation describing the beam deflection *w(x, t)* reads

$$EI\frac{\partial^4 w(x,t)}{\partial x^4} + \rho A\frac{\partial^2 w(x,t)}{\partial t^2} = q(x, t) \qquad (2.1)$$

where *EI* is the bending stiffness of the beam, ρ is density, *A* is cross-sectional area, giving $\rho A = m$, which is the mass of the beam per meter (kg/m), and *q(x, t)* is the load on the beam (*t* is time).

The beam is supported at the ends only, i.e., at x = 0 and x = L (beam length L is assumed).

Damping of the beam is not included in this model. For stationary vibrations of the undamped beam, the solution to (the homogeneous part of) this equation may be written in the form

$$w_{hom}(x, t) = X(x)T(t) = X(x)\sin \omega t \qquad (2.2)$$

where *X(x)* gives the form of the beam deflection when it vibrates (the vibration mode) and ω is the vibration angular frequency.

Rayleigh-Timoshenko Beam (R-T beam)

The R – T beam theory includes rotatory inertia and shear deformation of the beam. In this case, two differential equations are needed to describe the vibrations. The deflection w(x, t) and the shear deformation ψ(x, t) are unknown functions. The differential equation for the deflection w(x, t) becomes

$$EI\frac{\partial^4 w(x,t)}{\partial x^4} + \rho A\frac{\partial^2 w(x,t)}{\partial t^2} - \rho I\left(1+\frac{E}{kG}\right)\frac{\partial^4 w(x,t)}{\partial x^2 \partial t^2} + \frac{\rho^2 I}{kG}\frac{\partial^4 w(x,t)}{\partial t^4} = q(x,t) + \frac{\rho I}{kGA}\frac{\partial^2 q}{\partial t^2} - \frac{EI}{kGA}\frac{\partial^2 q}{\partial x^2}$$

where EI, ρ, A, and $q(x, t)$ are the same as in the E-B case, G is the shear modulus, and k is the shear factor. Also, this equation (like the E-B one) describes the behaviour of the beam between the supports at the beam ends. A similar equation is obtained for the shear deformation ψ(x, t).

If the shear deformation of the beam is suppressed, i.e., if one gives k a very large value, then the two last terms on both sides tend to zero. Further, if the mass inertia in rotation of the beam cross section is eliminated (noting that $\rho I = \rho r^2 A = mr^2$, and let r tend to zero), then the third term also tends to zero and the E-B differential equation is obtained.

It was found that shear deformation of the rail can be neglected only for frequencies below 500 Hz. Dahlberg showed that at this frequency (500 Hz), and for a UIC60 rail, the Euler-Bernoulli beam theory provides a vibration frequency that is 10 to 15% too high. [4]

2.3.2 Railpads and fastening

The most commonly used physical model of a railpad is the spring-damper system. The spring is usually assumed to be linear, and the damping is assumed to be proportional to the deformation rate of the railpad.

In the measurements carried out on influence of soft and stiff railpads on the wheel-rail contact force and the track dynamics, soft railpads were found to result in lower sleeper acceleration and higher railhead acceleration than the stiff railpads.

The role of the fastenings is normally neglected when investigating track dynamics. The stiffness of the fastening is normally much less than that of the railpad. Therefore, when a wheelset loads the track, only the railpad stiffness is important. For an unloaded rail, however, the fastening will induce a certain preload (static load) on the railpad, and, knowing that the railpad stiffness is nonlinear, this may influence the dynamics of the unloaded track.

2.3.3 Sleepers

Depending on which frequency interval is of interest, the concrete sleeper can be modelled as either a rigid mass (at frequencies below 100 Hz) or as a flexible beam. For frequencies up to 300 or 400 Hz, the Euler-Bernoulli beam theory may suffice. At higher

frequencies, the Rayleigh-Timoshenko beam theory should be used for an accurate description of the sleeper vibration.

Along the rail, the stiffness changes because it is supported by sleepers separated by a distance around 65 cm. The stiffness is higher when the wheel passes at the level of a concrete sleeper. These vibrations induced by the sleeper distance have a frequency *f* given by the equation where *V* is the speed of the train and *D* is the distance between two sleepers. [4][5]

$$f = \frac{V}{D} \qquad (2.4)$$

2.3.4 Ballast, subballast and subgrade

Ballast is a complex medium because of its granular properties. The ballast is constituted by stone particles. The behaviour of the ballast is not well-known because of the complexity of the interactions between particles. A granular media can have behaviour both like solids and liquids: on one hand, the ballast supports sleepers; on the other hand, the liquefaction of ballast is a dangerous problem which can cause derailment. Without any train loadings, internal forces in the ballast are low. During train passages, the friction between particles increases and the ballast is compressed by the train loading.

At present, the state-of-the-art of track design concerning the ballast and the subgrade is mostly empirical. The factors that control the performance of the ballast are poorly understood. No generally accepted damage and settlement equations or any material equations for the ballast itself have been found. Only different suggestions to describe the ballast settlement from a phenomenological point of view are available. A historical method for assessing track performance is the use of track modulus. [4][5]

2.4 Track Forces

Types of forces imposed on the track structure are classified as mechanical, both static and dynamic and thermal. The track structure must restrain repeated vertical, lateral and longitudinal forces resulting from traffic and changing temperature. [1]

The requirements for the bearing strength and quality of the track depend to a large extent on the load parameters: axle load (static vertical load per axle), tonnage borne as the sum of the axle loads and the running speed.

The static axle load level, to which the dynamic increment is added, in principle determines the required strength of the track. The dynamic load component which

depends on speed and horizontal and vertical track geometry also plays an essential part here. [6]

The forces acting on the track as a result of train loads are considerable and sudden and are characterised by rapid functions. The loads can be considered from three main angles: vertical, lateral and longitudinal forces.

Vertical force

Vertical forces are considered those that are perpendicular to the plane of the rails. As such, the actual direction is a function of the track cross-level and grade. The types of vertical forces are vertical wheel force and uplift force.

In reaction to the vertical downward force on the rail at the wheel contact point, the rail tends to lift up away from the wheel, as shown in Fig. 2-2. If the uplift force is not compensated by the rail and sleeper weight together with any frictional force from the ballast, the sleeper will lift momentarily. With the advancing of the wheel the particular sleeper is forced down. This movement causes a pumping action which can cause deterioration of track structure components. [1]

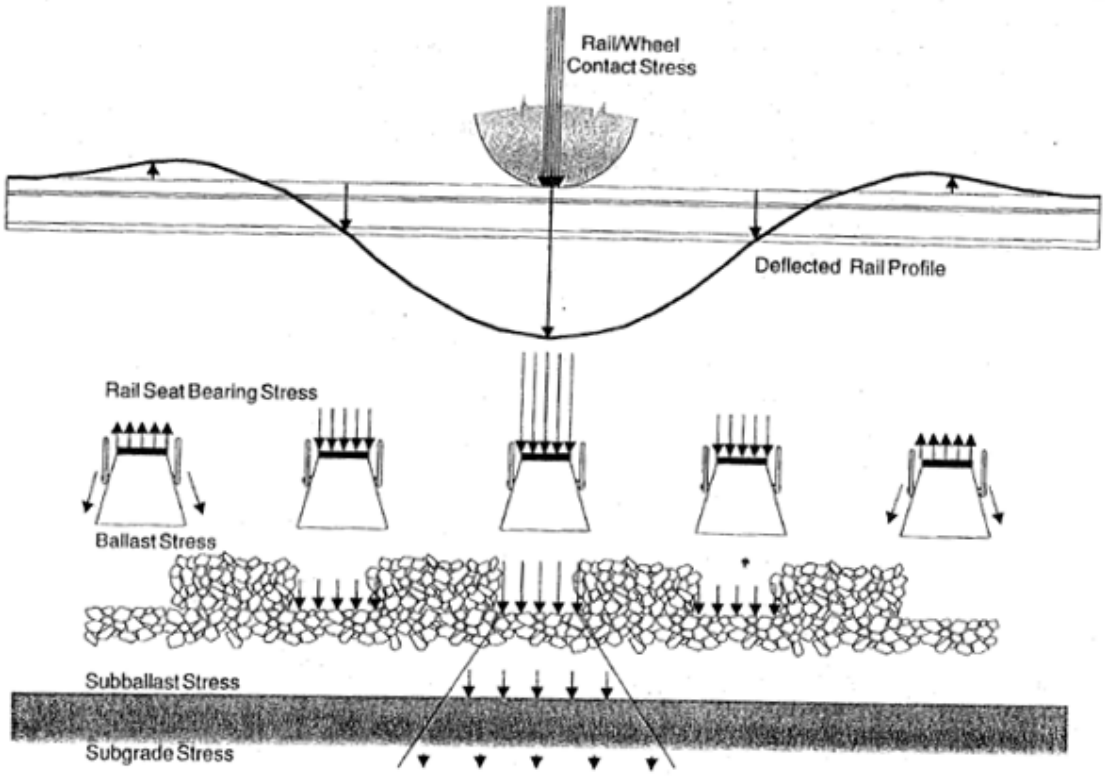

Figure 2-2 Typical wheel load distribution into the track structure [1]

The vertical wheel force is often considered as having a static component equal to the vehicle weight divided by the number of wheels plus a dynamic variation about the static value.

Sources of vertical dynamic variation are track geometry induced vehicle-rail interaction including rock and roll and bounce; and wheel impact forces from causes such as wheel flats, rail burns, rail corrugations and rail joints.

2.5 Modelling for dynamic loading

The dynamics of the compound train and track system plays an important role when investigating vehicle and track dynamics. Vibrations may lead to track deterioration, such as railhead corrugation growth, damage to track components (railpads, sleepers, ballast), track settlement, and so on.

Techniques to study the train-track interaction can be divided into two groups: frequency-domain techniques and time-domain techniques. [4][7]

2.5.1 Frequency domain modelling

In the frequency-domain technique, receptances of the track are required. If a stationary (not moving) wheel is loading the track, then the track receptance is needed only at the point where the wheel is situated. The receptance (vertical or lateral, depending on what is studied) may be measured *in situ* on the track or it can be calculated using a track model. If a harmonically varying stationary load excites the track, then the direct receptance provides the track response.

Using the frequency-domain technique it is possible to investigate the track and wheel response to a "moving irregularity". Instead of a having a wheel moving on an un-even rail, one investigates a stationary wheel. The rail and the (stationary) wheel are then excited at the wheel-rail contact patch by a prescribed displacement.

One may think of this excitation as if a strip of irregular thickness were inserted between the wheel and the rail. The strip is then forced to move between the wheel and the rail so that the irregularity of the strip will excite both wheel and rail. The response of the wheel and the track is obtained in the frequency domain.

If a continuously supported rail is excited by a harmonically varying moving load, then the track response can be determined in a coordinate system following the load.

The response is then assumed to be stationary. One method to treat a discretely supported rail is to develop the support reactions into Fourier series (making the support continuous but non-uniform) and then the moving load problem is solved with respect to a coordinate system following the load.

In the frequency-domain technique only fully linear systems can be treated. The track responses are also assumed to be stationary, implying that singular events along the track, such as a rail joint, a sleeper hanging in the rail (no support from the ballast), varying track stiffness, and so on, cannot be treated.[4][7]

2.5.2 Time-domain modelling

When train-track dynamics is investigated in the time domain deflections of the track and displacements of the vehicle are calculated by numerical time integration as the vehicle moves along the track. The vertical motion of the wheelset should then coincide with the vertical deflection of the rail, while taking the wheel-rail contact deformation into account. The wheel-rail contact force is unknown and has to be determined in the calculations.

The track can be modelled by finite elements and in many cases a modal analysis of the track is performed. The track is then described through its modal parameters, and the physical deflections of the track are determined by modal superposition. Often the vehicle is modelled by use of rigid masses, springs (linear or non-linear) and viscous dampers. If a more detailed response of the vehicle is of interest, then it could be convenient to use modal analysis also for the vehicle deformations (the vehicle is no longer composed of rigid bodies). The modal analysis technique requires linear models. Every so often track models may comprise also non-linear track elements. [4][7]

2.6 Mathematical modelling of track dynamics

As stated by [2], models of track dynamic behaviour may be generally classified into two categories:

- those that represent the track as a continuously supported rail beam and
- those that represent the track as a discretely supported rail beam

Continuously supported models of infinite length are based on the beam on elastic foundation theory.

The rail, pads, fastenings, sleepers, ballast, sub-ballast and subgrade are components that define the value of the modulus of track elasticity.

Discretely supported models are similar to the continuously supported models and often have multiple layers representing the rail pads, sleepers, ballast, subballast and subgrade.[2]

2.6.1 Beam (rail) on continuous elastic foundation (Winkler Beam)

The rail may be modelled either as an ordinary Euler-Bernoulli beam (the conventional beam theory is used) or as a Rayleigh-Timoshenko beam.

The Rayleigh-Timoshenko beam theory includes the rotatory inertia of the beam cross section and beam deformations due to the shear force. Also, a longitudinal (axial) force in the rail may be included in these models.[4]

In the most simple track model, a beam (that is a model of the rail) rests on a continuous elastic foundation. The foundation is modelled by an evenly distributed linear spring stiffness. The distributed force supporting the beam is then proportional to the beam deflection.

The only track parameters needed for this model are the beam bending stiffness EI (Nm^2) and the foundation stiffness (the bed modulus) k (N/m^2, i.e., N/m per meter of rail). The rail deflection *w(x)* (x is the length coordinate) is then obtained from the differential equation:

$$EI\frac{d^4w}{dx^4} + kw(x) = q(x), \qquad (2.5)$$

where *q(x)* is the distributed load on the rail

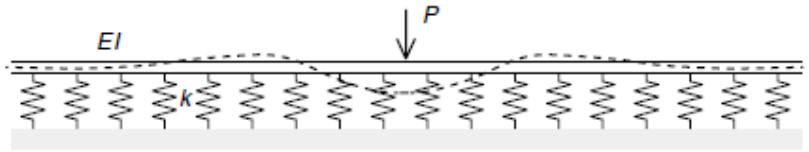

Figure 2-3 Beam (bending stiffness EI) on elastic foundation (bed modulus k) [4]

2.6.2 Beam (rail) on discrete supports

The supports in this model could be either discrete spring-damper systems or spring-mass-spring systems, modelling railpads, sleepers and ballast bed. One commonly used method to model this is to place the rail (a beam) on a spring and a damper in parallel. This spring-damper system models the railpad, below which is placed a rigid mass

modelling the sleeper. The sleeper rests on an elastic foundation, i.e., another spring-damper system.

Sometimes, the rigid sleeper mass is replaced by a beam on an elastic foundation. The beam then extends perpendicularly to the rail, and the track model becomes three-dimensional.

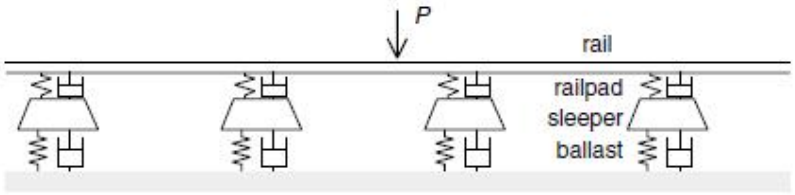

Figure 2-4 Rail on discrete supports[4]

2.6.3 Discretely supported track including ballast mass

To be able to add a resonance frequency at low frequency (20 to 40 Hz) to the model described above, more masses are incorporated into the model Fig 2-5.

By making the ballast and subgrade mass large (much larger than the sleeper and rail mass) and by adjusting the subgrade stiffness, a resonance at low frequency can be achieved. Then, essentially, the ballast-subgrade masses vibrate on the subgrade stiffness. It is noted in Figure 2-5 that there are connections between the ballast and subgrade masses, implying that a deflection at one point (at one sleeper) will influence the deflection at the adjacent sleepers. This phenomenon (which exists in a real track) cannot be modelled with the simpler models such as the track model in Fig 2-4.[4]

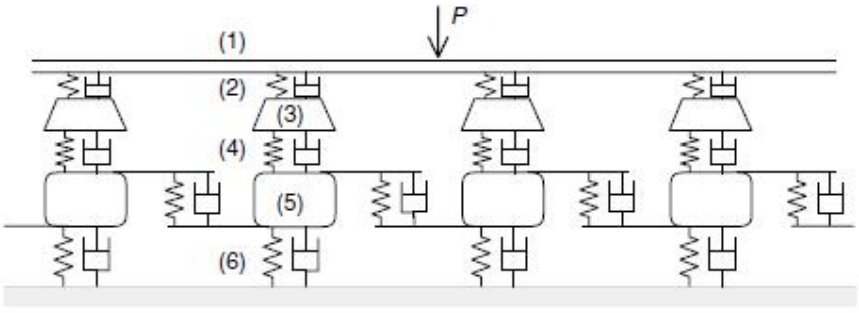

Figure 2-5 Rail on discrete supports with rigid masses modelling the sleepers[4]

(1) Rail, (2) railpad stiffness and damping, (3) rigid sleepers, (4) ballast stiffness and damping. Rigid masses (5) below the sleepers represent the mass of the ballast and the subgrade, (6) subgrade stiffness and damping.

By this model, the four resonance vibration modes (a) embankment vibration, (b) track-on-the-ballast vibration, (c) rail-on-railpad vibration, and (d) pinned – pinned vibration of the rail, may be captured.

2.6.4 Rails on sleepers embedded in continuum. Three-dimensional finite element models

The most realistic track model, and the model that normally requires the most computer capacity, is the model where rails and sleepers are modelled as beams (or possibly as three-dimensional bodies) with elastic elements modelling the railpads between the rails and the sleepers. The sleepers are embedded in a continuous medium. This requires that the track bed is modelled by three dimensional finite elements. Figure 2-6 shows such a track model. Using a model like this, and also modelling a larger part of the surroundings, wave propagation from the track to the surroundings can be simulated. In the small model in Figure 2-6, non-reflecting boundary conditions must be used to avoid wave reflections at the boundaries. [4]

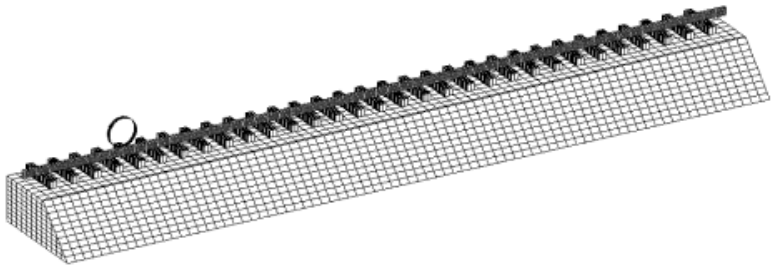

Figure 2-6 Rail on sleepers and the sleepers are embedded in a continuous ballast and subgrade medium[4]

2.7 Deterioration of Track

Deterioration or degradation is the reduction of the original quality due to various influences. By far the most significant factor contributing to the deterioration is the dynamic load. The dynamic load is directly related to the axle load and track geometry.
The main processes of track deterioration are [2]

- wear
- fatigue and
- settlement

Three main groups of factors may be distinguished that contribute to the deterioration of railway infrastructure:

- Use: wear by physical contact, static and dynamic load
- Environment: climatic influence, water
- Failures**:** faulty components, bad construction

In most of the cases it is not just one of these factors that causes deterioration, but a combination of them.

2.7.1 Parameters affecting track deterioration

2.7.1.1 Driving forces of deterioration

A railway track is designed to distribute the loads from trains down to the soil/ground. This distribution through superstructure and substructure depends on original track design and current track condition. Stiffness of different components in the track structure, as well as the resulting (global) track stiffness will partly determine how the loads are distributed. The static, quasi-static and dynamic forces are all important for track degradation. Some aspects determining forces and thereby influence degradation are listed in the following table. [2]

Table 2-1 Parameters influencing track degradation [2]

Subsystem	Characteristics	Influence of the Subsystem
Vehicle	• speed, • axle load, • unsprung mass, • suspension, • wheel profile, • axle spacing etc.	• static, • quasi-static and • dynamic forces
	• Wheel (current condition such as wheel flats and wheel corrugation)	• dynamic forces
Track	• Track design geometry (curves etc.)	• static and • quasi-static forces
	• Track geometry quality	• dynamic forces
	• Corrugation	• high-frequency forces
	• Rail imperfections such as joints or poor welds	• impact forces

2.7.1.2 Dynamic effects

Traffic on rail lines comprises many different forms of vehicle, varying from high speed passenger units (electric and diesel), to medium speed wagons and locomotives, to lower speed mixed freight consists. Track is therefore subject to a wide range of bearing and bending stresses in the rails, pads, fasteners, sleepers, ballast and subgrade. [8]

These stresses come about because of

- the static mass of a vehicle, its wheel sets and the cargo (freight or passenger)
- the dynamic actions such as
    - lateral centrifugal forces on curves,
    - longitudinal acceleration and braking forces,
    - rocking of the vehicle about 3 axes (roll, pitch and yaw),
    - vertical inertial forces from the motion of the wheel set and its suspension,
    - vibration forces induced from imperfections in the rail surface (corrugations, joints, welds, defects) and in the wheels (flats and shells) and
    - the dynamic response of the track components to these actions.

The consequences of the frequently large forces generated by these actions are many and varied. The major deleterious effects are

- fatigue cracking in rails,
- plastic flow or shelling out of the rail head,
- uneven wear of the rail head,
- cracking or splitting of sleepers,
- loosening of fasteners,
- grinding and redistribution of ballast and
- variations in track alignments and gauge

Such effects result in poor riding quality, reduced train speed, increased fuel consumption, potential derailment, increased maintenance, delays and reduced level of service, and loss of revenue in the longer term. [8]

2.7.1.3 Train speed

For a long period, train loads have been believed to be reasonably assumed as quasi-static moving loads. Studies considered that a train will encounter the 'sound barrier'

(critical speed) when reaching the velocity of Rayleigh surface waves propagating in the ground. [9]

The critical condition is explained as resonance between the moving train and the Rayleigh wave of the subgrade soil. This phenomenon can be compared with the Mach effect by supersonic jets and the Cherenkov radiation of light.

Depending on whether the speed of a moving train is less than, great than or close to the velocity of Rayleigh wave, the train speed effect can be categorized as subsonic, supersonic and transonic. When a train runs at a speed less than the Rayleigh wave velocity, the ground vibrations behave and represent a quasi-static condition. The increase in vibration magnitude is slow relative to increase in train speed. However, under transonic and supersonic cases, the dynamic effects of ground vibrations perform like the development of Mach lines and Mach surfaces. Vibration magnitude increases exponentially with train speed. Critical speed is defined as the speed at which moving trains resonate with waves travelling in the track and produce excessive ground vibrations. [9]

Increasing the speed of trains has many effects on rail and track behaviour and degradation, and has long been considered in regard to the level of noise and vibration experienced near rail lines. Higher speeds cause greater track deflections, and the speed of a train can significantly influence the deterioration of track geometry. The speed may not influence dynamic vertical wheel loads.

Studies on the profile of track showed that large vertical wavelength deviations of the rail top produced dynamic forces which varied widely depending on the speed of a train. Furthermore, analytical models have shown that vehicle speed is one of the key factors affecting the wheel/rail impact loads; these loads produce very high bending stresses in rails and in sleepers (except where attenuated by resilient pads), and can lead to fatigue and/or cracking in vehicle axles and bearings. [8]

Railway transport networks have been regaining their importance in recent decades, which has led to increasing train speeds, higher axle loads and more frequent train usage. Table 2-2 shows the speed record for conventional trains in the last decade. [10]

Table 2-2 Some speed record for conventional trains [10]

Speed	Year	Country	Train
210 km/h	1903	Germany	AEG
230 km/h	1931	Germany	Schienenzeppelin
331 km/h	1955	France	Aboard Train V150
380 km/h	1981	France	TGV
407 km/h	1988	Germany	ICE
515 km/h	1990	France	TGV-A
575 km/h	2007	France	TGV

2.7.1.4 Axle loads

Many railways were built to accommodate set axle loads for freight cars and locomotives, calculated as tons per axle; raising this limit is an effective way to increase rail system capacity. [11]

Technical factors that limit axle loads include type, size, and spacing of sleepers; rail weight or size; thickness of roadbed sections; rail metallurgy; and bridge and culvert designs.

Some railways have low axle load limits of 12.5 tons/axle. Typical heavy-duty railways have at least 25-tons/axle limits; North American railways have 32.5tons/axle limits, a level common to heavy-haul railways in many countries. Recently, an Australian company built a specialized mineral railway designed for 40-tons/axle loads, which is currently the upper load limit for railways due to rail metallurgy limitations.

Increasing axle loads significantly boosts railway capacity because higher axle loads increase freight car carrying capacity almost directly, without increasing the weight of the freight cars very much, if at all. For example, increasing axle load limits from 22.5 to 25 tons (about 10%) increases the carrying capacity of a fully loaded freight car from about 68 tons to 78 tons (a 15% increase). [11]

Axle loads affect rail head wear, fatigue of the rail steel and plastic flow and shelling in the running surface between wheel and rail head. Greater axle loads lead to increased wheel wear and higher bending stresses in rails and sleepers, as well as higher bearing stresses in ballast and subgrade.

Studies on the effect of increased axle load on the track maintenance have shown that, routine maintenance demands were 60% greater for a 20% increase in axle load and a 9% increase in axle load led to a 14% increase in total track costs. [8]

2.8 Overview of Prestressed Concrete Sleepers

2.8.1 Prestressing

Reinforced concrete is the most widely used structural material of the 20th century. Because the tensile strength of concrete is low, steel bars are embedded in the concrete to carry all internal tensile forces. Tensile forces may be caused by imposed loads or deformations, or by load-independent effects such as temperature changes or shrinkage.

Prestressed concrete is a particular form of reinforced concrete. Prestressing involves the application of an initial compressive load on a structure to reduce or eliminate the internal tensile forces and thereby control or eliminate cracking. The initial compressive load is imposed and sustained by highly tensioned steel reinforcement reacting on the concrete. With cracking reduced or eliminated, a prestressed section is considerably stiffer than the equivalent (usually cracked) reinforced section. Prestressing may also impose internal forces which are of opposite sign to the external loads and may therefore significantly reduce or even eliminate deflection. [12]

2.8.1.1 Prestressing systems

Prestress is usually imparted to a concrete member by highly tensioned steel reinforcement (wire, strand, or bar) reacting on the concrete.

The high strength prestressing steel is most often tensioned using hydraulic jacks. The tensioning operation may occur before or after the concrete is cast and, accordingly, prestressed members are classified as either pre-tensioned or post-tensioned. [12]

Pre-tensioning

The term pretensioning means pretensioning of the prestressing steel, not the beam it serves.[13] The prestressing tendons are initially tensioned between fixed abutments and anchored. With the formwork in place, the concrete is cast around the highly stressed steel tendons and cured. When the concrete has reached its required strength, the wires are cut or otherwise released from the abutments. As the highly stressed steel attempts to contract, the concrete is compressed. Prestress is imparted via bond between the steel and the concrete. Pretensioned concrete members are often precast in pretensioning beds long

enough to accommodate many identical units simultaneously. To decrease the construction cycle time, steam curing may be employed to facilitate rapid concrete strength gain and the concrete is often stressed within 24 hours of casting. [12]

Prestressing can be accomplished by prestressing individual strands or all the strands at one jacking operation. [13]

a)

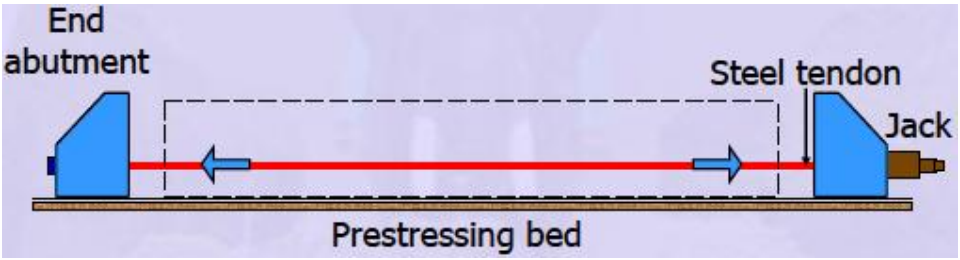

b)

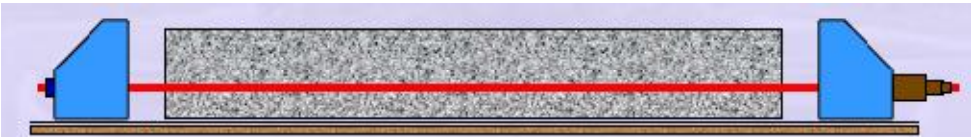

c)

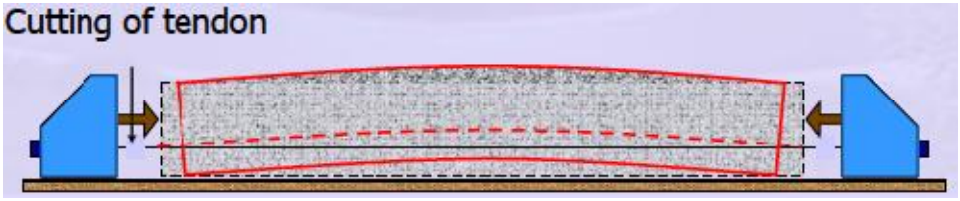

Figure 2-7 Stages of pretensioning a) Applying tension to tendons, b) Casting of concrete and c) Transferring of prestress [14]

2.8.1.2 Advantages of prestressed concrete

Prestressed concrete offers great technical advantages in comparison with other forms of construction, such as reinforced concrete and steel. In the case of fully prestressed members, which are free from tensile stresses under working loads [15]

- The cross-section is more efficiently utilized when compared with a reinforced concrete section which is cracked under working loads.

- Prestressed concrete members possess improved resistance to shearing forces, due to the effect of compressive prestress, which reduces the principal tensile stress.
- A prestressed concrete flexural member is stiffer under working loads than a reinforced concrete member of the same depth.
- The use of high-strength concrete and steel in prestressed members results in lighter and slender members than is possible with reinforced concrete.
- In the long span range, prestressed concrete is generally more economical than reinforced concrete and steel.
- Prestressed concrete has considerable resilience due to its capacity for completely recovering from substantial effects of overloading without undergoing any series damage. [15]

2.8.2 Advantages and drawbacks of concrete sleepers

The development and use of concrete sleepers became significant after the Second World War owing to the scarcity of wood, the introduction of CWR track and the improvements in concrete technology and prestressing techniques. [6]

Specific advantages and drawbacks of concrete sleepers are:

Advantages

- Heavy weight, useful in connection with stability of CWR track
- Long service life provided fastenings are good or can be replaced easily
- Great freedom of design and construction
- Relatively simple to manufacture
- Concrete sleepers are neither inflammable nor subjected to damage by pests or corrosion under normal circumstances [16]
- Concrete sleepers have a very long lifespan, probably 40–50 years [16]

Disadvantages

- Less elastic than wood and on poor formation pumping may occur
- Susceptible to corrugation and poor quality welds
- Risk of damage from impacts(derailment, loading/unloading, tamping)
- Dynamic loads and ballast stresses can be as much as 25% higher
- Residual value is negative

- Handling and laying concrete sleepers is difficult due to their large weights[16]

2.8.3 Types of concrete sleepers

There are two basic types of concrete sleepers such as twin-block and monoblock sleepers.

2.8.3.1 Monoblock concrete sleeper

This is based on the shape of a beam and has roughly the same dimensions as a timber sleeper. It can be pretensioned or post-tensioned. [6][17]

Advantages

- little susceptibility to cracking
- can be prestressed
- give better longitudinal and lateral stability to the track
- distribute loads better than twin-blocks
- provide a good surface for the maintenance inspection staff

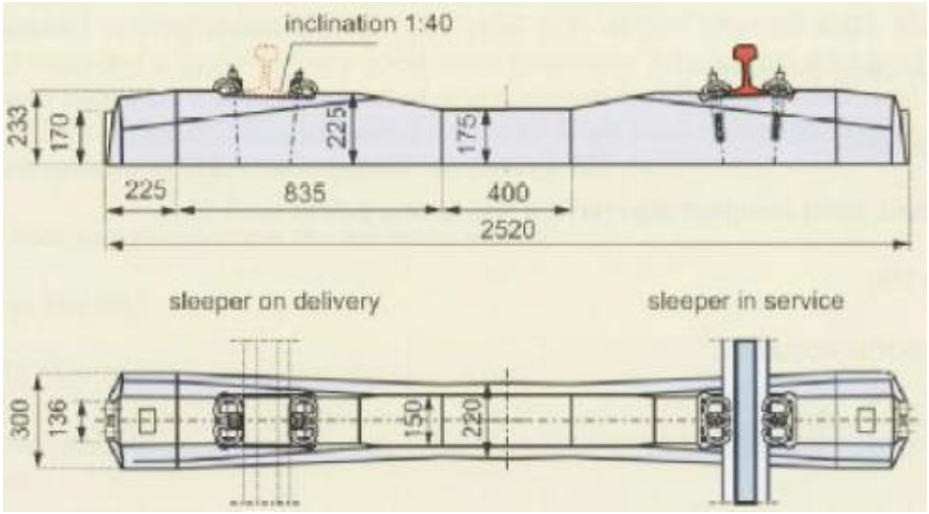

Figure 2-8 Prestressed monoblock sleeper [6]

Disadvantages

- transverse resistance is lower than that of twin-blocks
- requires heavy capital expenditure for its manufacture

2.8.4 Design considerations

When designing a sleeper, an evaluation of the loads being transferred and their flow through the track structure is essential. Therefore, forces and pressures of interest include

the rail seat load, lateral load, and the ballast pressure. The required flexural capacity is determined based on the ballast support conditions (pressure distributions) encountered during the life of a tie and the applied rail seat loads. AREMA has accounted for these various loading and support conditions in the minimum specified positive and negative moments located at the critical sections of the rail seat and tie centre. Similarly, lateral loads are accounted for in tie and fastener design. Fasteners are designed for the transfer of a minimum lateral load to account for those encountered in curved sections of track, while ties must be capable of withstanding lateral loads to maintain horizontal track geometry. [18]

2.8.4.1 Railseat load

As a train moves along the track, the load from an axle is distributed amongst several ties due to the rigidity of the track. A single tie typically carries between 45 to 65 percent of an axle load directly above it. Factors affecting this load distribution are the tie spacing, fastening system, rail stiffness, and ballast and sub-grade conditions with tie spacing having the largest effect. Typical track design with concrete ties utilizes tie spacing between 19 in and 27 in.

In the past, equations and variables were used to calculate the rail seat load; however, to simplify the process of calculating rail seat loads, AREMA collected the factors related to the load distribution and created a design aid relating the percentage of a wheel load transferred to a single tie as a function of tie spacing. For example, a tie spacing of 24 in would correlate to approximately 50 percent of the applied axle load being carried by that particular tie. Additionally, to account for rail irregularities and dynamic wheel load effects, impact factors are applied. Typical impact factors are 200 percent of applied static wheel loads. [18]

2.8.4.2 Ballast support reaction

When track is freshly tamped the contact area between the sleeper and the ballast occurs below each rail seat. After the tracks have been in service the contact pressure distribution between the sleeper and the ballast tends towards a uniform pressure distribution. This condition is associated with a gap between the sleeper and the ballast surface below the rail seat. The condition of centre binding of concrete sleepers tends to develop when maintenance is neglected. [19]

Ballast support is crucial to a tie's ability to support load. Poor ballast support results in tie cracking and eventually flexural failure.

During service, it is essential that the ballast and sub-grade are not over stressed. In reality pressure between the tie and ballast is not uniform across the bottom of the tie, but an approximation or average is used to limit bearing pressures and prevent excessive depression of the track. This average ballast pressure is a function of the applied axle loads, impact factors and the bearing area of the tie. [20]

Various hypothetical contact pressure distributions between the sleeper and the ballast are presented in Table 2-3.

Table 2-3 Hypothetical distribution of sleeper bearing pressure (Current practices) [19]

Item No.	Distribution of bearing pressure	Developers	Remarks
1		ORE Talbot	Laboratory test
2	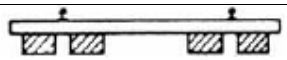	ORE, Talbot, Battelle, Clarke	Tamped either side of rail
3		ORE, Talbot	Principal bearing on rails
4	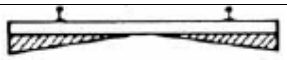	ORE, Talbot	Maximum intensity at ends
5		Talbot	Maximum intensity in middle
6	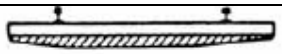	Talbot	Centre bound
7	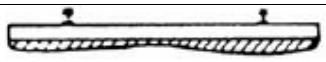	Talbot	Flexure of sleeper produces variations form
8	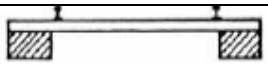	ORE, Talbot, Kerr, Schramm	Well tamped sides
9		ORE, Talbot	Stabilized rail seat and sides
10	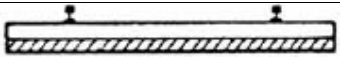	AREA, Raymond, Talbot	Uniform pressure

2.8.5 Failure mechanism of concrete sleepers

According to [18] the three primary failure mechanisms of concrete sleepers observed by the rail industry today are rail seat abrasion, flexural cracking from centre binding and rail fastener failure. Of these three, rail seat abrasion is the most common and difficult to prevent. Failures may be related to concrete tie materials, design or a combination of the two. Installation and maintenance practices also contribute to a tie's resistance to these failure mechanisms. A discussion of the three primary failure mechanisms is presented in the following sections.

2.8.5.1 Rail seat abrasion

The most common failure mode in the modern prestressed concrete railroad tie is rail seat abrasion. Rail seat abrasion is the gradual wearing away of the cement paste from the concrete, resulting in an uneven aggregate bearing surface beneath the tie pad. Factors contributing to rail seat abrasion include: the presence of water, high tonnage, steep track grades, and especially track curves greater than two degrees.

To prevent rail seat abrasion and prolong tie life, concrete tie manufactures have investigated methods to protect concrete in the rail seat region. Research has focused on the application of abrasion resistant materials applied in the form of pads, adhesive polymers (epoxy and polyurethane) or cast-in-place plates in the rail seat region. Some industry techniques used to mitigate rail seat abrasion to date include:

- Epoxy or polyurethane applied to rail seat shortly after casting,
- Cast-in-place steel plates,
- 3-part abrasion resistant pad assembly.

Of these options, epoxy or polyurethane has shown promising short term results and appears to have gained acceptance among manufacturers and railroads. However, epoxy and polyurethane do wear down over time allowing rail seat abrasion to take place. For rail seat abrasion repair operations, the application of epoxy is common, but requires specific temperature and humidity control and also results in costly track closures. Testing of cast-in-place steel plates has shown no rail seat abrasion at 4 times the number of cycles required to cause failure of currently used tie designs. However, issues with water intrusion below the plate and the additional cost of materials and fabrication have limited the use of the cast-in-place steel plate method. 3-part abrasion resistant pad

assemblies remain the industry standard due to lower initial cost and ease of replacement. [18]

2.8.5.2 Flexural cracking (centre binding)

Investigations have shown that this failure type results from ballast conditions which are beyond the scope of tie design. Over time cyclic loading applied to the track causes ties to oscillate and deform vertically within the track structure; this deformation produces pumping action which ultimately allows ballast to abrade the bottom of the tie and pulverize the ballast beneath the tie.

The pulverized ballast is routinely removed from the track and replaced with new ballast during undercutting maintenance operations. However, when undercutting and replacement is not carried out regularly, depressions in the pulverized ballast beneath the ends of the tie may develop, altering the support condition of the tie. The new support condition is a centre support where ballast bearing still remains. Based on this support condition the tie cantilevers from the centre over the pulverized ballast depression. When loaded, large negative moments occur at the tie centre, resulting in cracking and tie failure as the flexural capacity is exceeded. This type of failure is referred to as “centre binding”. To prevent centre binding regular maintenance of ballast must be performed to avoid deterioration of the material leading to unsuitable tie support conditions.

2.8.5.3 Fastener failure

Due to the effect of cyclic loading, fatigue of fastener components such as the spring clip and embedded ductile iron shoulder occurs which allows for movement of the rail, deterioration of pads, and a decrease in the fastener toe load applied to the rail.

In addition to a decreased toe load, polymer insulators located between the rail and spring clip are subjected to abrasion from cyclic loading. Over time this abrasion wears away insulating material, creating voids and allowing for excess movement between the rail-tie interface in the form of rail rocking side to side and slip in the longitudinal direction of the rail. This excess movement and space between the tie and rail further exacerbates the related issue of rail seat abrasion by providing an abrasive motion and allowing for the intrusion of water and abrasive agents such as rail grit or coal dust.

To prevent fastener failure or related issues such as rail seat abrasion regular maintenance of fastener components is essential. The replacement of worn insulators and

other components can prevent escalation of further issues before they begin. Fastener wear is relatively easy to monitor visually compared to rail seat abrasion which is typically hidden by the rail and ballast. It should also be noted that fastener fatigue requires long periods of time and is typically a secondary failure mechanism when compared to the rail seat abrasion and centre binding failures. [18]

CHAPTER 3 FINITE ELEMENT MODELLING

3.1 Introduction

The FEM was first used to solve problems of stress analysis, and has since been applied to many other problems like thermal analysis, fluid flow analysis, piezoelectric analysis, and many others. Basically, the analyst seeks to determine the distribution of some field variable like the displacement in stress analysis, the temperature or heat flux in thermal analysis, the electrical charge in electrical analysis, and so on. [21]

The FEM is a numerical method seeking an approximated solution of the distribution of field variables in the problem domain that is difficult to obtain analytically. It is done by dividing the problem domain into several elements. Known physical laws are then applied to each small element, each of which usually has a very simple geometry. A continuous function of an unknown field variable is approximated using piecewise linear functions in each sub-domain, called an element formed by nodes. The unknowns are then the discrete values of the field variable at the nodes. Next, proper principles are followed to establish equations for the elements, after which the elements are 'tied' to one another. This process leads to a set of linear algebraic simultaneous equations for the entire system that can be solved easily to yield the required field variable. [21]

3.2 Finite Element Modelling of Sleeper and Track

3.2.1 Sleeper cross-section

The vertical loads subject the sleeper to a bending moment which is dependent upon the condition of the ballast underneath the sleeper. The performance of a sleeper to withstand lateral and longitudinal loading is dependent upon the sleeper's size, shape, surface geometry, weight and spacing. [5]

The sleeper used for modelling is Chinese Type II sleeper which is currently being in use for national railway lines of Ethiopia. The detailed drawing and dimensions are shown in Figure 3-1.

(a)

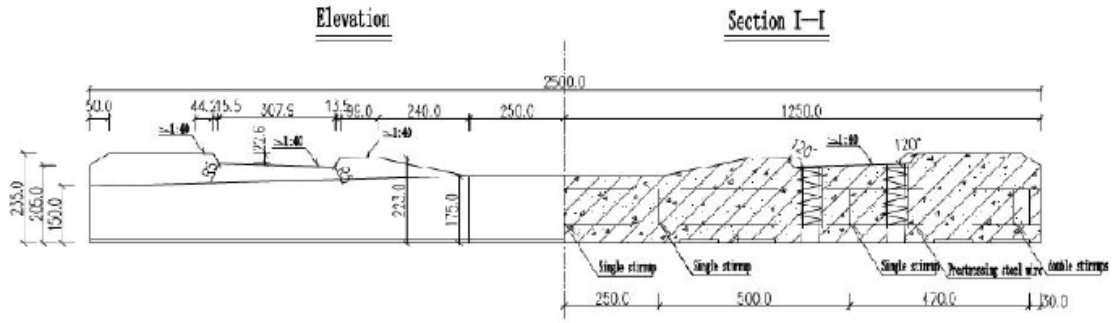

(b)

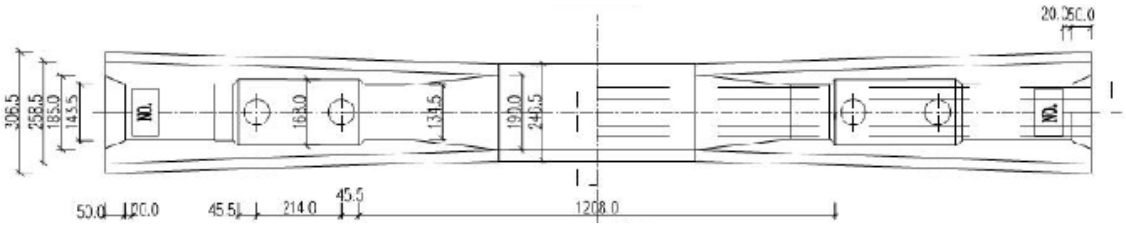

Figure 3-1 Type II sleeper drawing (a) Elevation (b) Plan [22]

3.2.2 Material property of concrete sleeper

As stated by [23], the concrete strength grade for prestressed concrete structures shall not be less than C30; concrete strength grade may not be less C40 when strand, steel wires and heat-treated steel reinforcements are used as prestressed steel reinforcement. Similarly, the code recommends stress-relieved steel wire (indented) with diameter of 5mm and 7mm for prestressing steel.

For concrete grade C60 (which is currently being used by ERC) and prestressing steel the material properties are listed in Table 3-1.

Table 3-1 Material properties of concrete and prestressing steel

No	**Properties of concrete**	**Value**
1	Density (ρ_c) kg/m^3	2400
2	Young's modulus (E_c) MPa	36000
3	Poisson's ratio (v_c)	0.2
4	Thermal expansion (α_c) / ℃	1*10^{-5}
	Properties of prestressing steel	
1	Density (ρ_s) kg/m^3	7850
2	Young's modulus(stress-relieved steel wire) (E_s) MPa	205000
3	Poisson's ratio (v_s)	0.3
4	Characteristic strength for prestressed steel wire (f_{ptk}) MPa	1570

The value of controlled stress for stretching prestressed reinforcement may not exceed the allowable value of controlled stress for stretching as stipulated in the Table 3-2 and shall be not less than 0.4 f_{ptk}. [23]

When there conforms to one of the following conditions, the allowable value of controlled stress for stretching in the Table 3-2 may be increased by 0.05f_{ptk}:

1. In order to increase the crack resistance in the construction stage for the members, it is required that the prestressed reinforcement shall be provided in the compression zone at service stage.
2. It is required to offset a part of the loss of prestress caused by the factors of stress relaxation, friction, batch stretching of steel reinforcement or the difference of temperature between the prestressed reinforcement and the stretching bed etc.

Table 3-2 Allowable value of controlled stress for stretching

Types of steel reinforcement	Method of stretching	
	Pre-tensioned	Post-tensioned
Stress-relief steel wire, strand	0.75f_{ptk}	0.75f_{ptk}
Heat-treated steel bar	0.70f_{ptk}	0.65f_{ptk}

Hence the value of stress for stretching prestressed reinforcement

$$\sigma = 0.75*1570 = 1177.5 \text{ MPa}$$

The initial strain of tendons can be obtained from the formula

$$\varepsilon = \frac{\sigma}{E} \qquad (3.1)$$

$$\varepsilon = \frac{1177.5}{205000} = 0.0057439 \text{ m/m}$$

Area of nominal ϕ5mm wire = $1.96349*10^{-5}$ m^2

3.2.3 Loading condition

3.2.3.1 Rail seat load

The functions of the sleepers are to transfer the vertical, lateral and longitudinal rail seat loads to the ballast and formation, and to maintain the track gauge and alignment by providing a reliable support for the rail fasteners. [5]

The nominal vehicle axle load is usually measured for the static condition, but in the design of railway track the actual stresses in the various components of the track structure and in the rolling stock must be determined from the dynamic vertical and lateral forces imposed by the design vehicle moving at speed.

The exact magnitude of the load applied to each rail seat depends upon the following known and unknown parameters: [5]

- the rail weight
- the sleeper spacing
- the track modulus per rail
- the amount of play between the rail and the sleeper
- the amount of play between the sleeper and the ballast

For the purpose of this thesis to find the rail seat load on the sleeper in the cases such as increasing train speed and axle load a three dimensional ballast track is modelled and transient wheel load is applied on the rail nodes for dynamic analysis. Then the maximum reaction force at rail seat is obtained.

3.2.3.2 Ballast pressure

Before the sleeper can be analysed in terms of its capacity to withstand the bending stresses caused by the vertical rail seat loads the sleeper support condition and its effect

upon the contact pressure distribution must be quantified. The contact pressure distribution between the sleeper and the ballast is mainly dependent upon the degree of voiding in the ballast under the sleeper. This voiding is caused by traffic loading and is due to the gradual change in the structure of the ballast and the subgrade. [5]

When the track is freshly tamped the contact area between the sleeper and the ballast occurs below each rail seat. After the track has been in service the contact pressure distribution between the sleeper and the ballast tends towards a uniform pressure distribution.

Before the contact pressure between the sleeper and the ballast can be calculated the following factors must be quantified: [5]

- the effective sleeper support area beneath the rail
- the maximum rail seat load occurring at a sleeper

In their study [22] considered two extreme cases: (i) total loss of contact in the central region (which occurs in the early life of the track structure) and (ii) full contact at all points (which occurs subsequently).

In AREMA[24], the contact pressure between tie and ballast for a well-maintained track is largest at the rail seat and smallest at the tie centre. This pressure distribution varies with accumulated traffic and track condition. In order to simplify the calculations, the dashed uniform distribution may be assumed, with $L_{eff} \cong L/3$ as shown in Figure 3-2. The bearing area of the tie is 2/3 of the footprint of the tie and the average intensity of pressure on ballast should not exceed 65 psi.

Then the effective bearing area of the tie is:

$$A_b = b*L_{eff} = 1/3(b*L) \quad (3.2)$$

where b = width of tie at base

The corresponding tie-ballast bearing pressure is

$$= \frac{3*Fdmax}{b*L} < 65\text{psi } (0.448\text{MPa}) \quad (3.3)$$

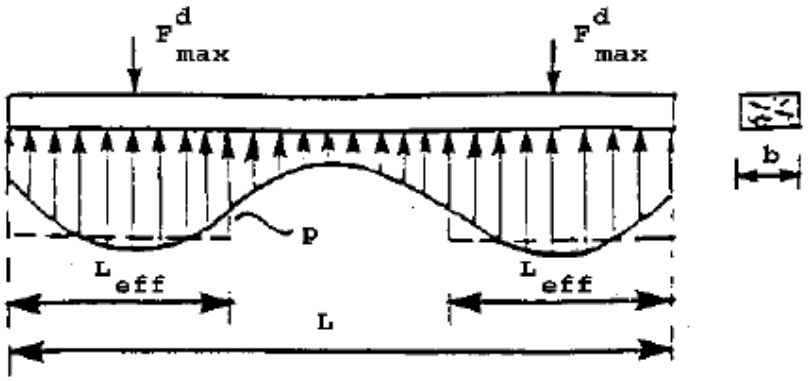

Figure 3-2 Pressure distribution [24]

In AREMA[24] it is also stated that while tie-to-ballast pressure is not uniformly distributed across or along the bottom of a cross tie, an approximate calculation can be made of "average" pressure at the bottom of the tie. The average pressure at the tie bottom is equal to axle load, modified by distribution and impact factors, and divided by the bearing area of the tie.

The effective bearing area of the tie is the entire footprint of the tie and the recommended ballast pressure should not exceed 85 psi (0.586 MPa) for high-quality, abrasion resistant ballast. If lower quality ballast materials are used, the ballast pressure should be reduced accordingly.

$$\text{Average Ballast Pressure, psi (MPa)} = \frac{(2P)\left[1+\frac{IF}{100}\right]\left(\frac{DF}{100}\right)}{A} < 85\text{psi (0.586MPa)} \qquad (3.4)$$

Where:

P = Wheel load in pounds (kN)

IF = Impact factor in percent

DF = Distribution factor in percent (from Figure 3-3)

A = Bearing area of cross ties in square inches (millimetres)

For the purpose of this thesis to determine the ballast pressure the above mentioned two cases are considered as Case 1($L_{eff} \cong 2L/3$) and Case 2 ($L_{eff} = L$).

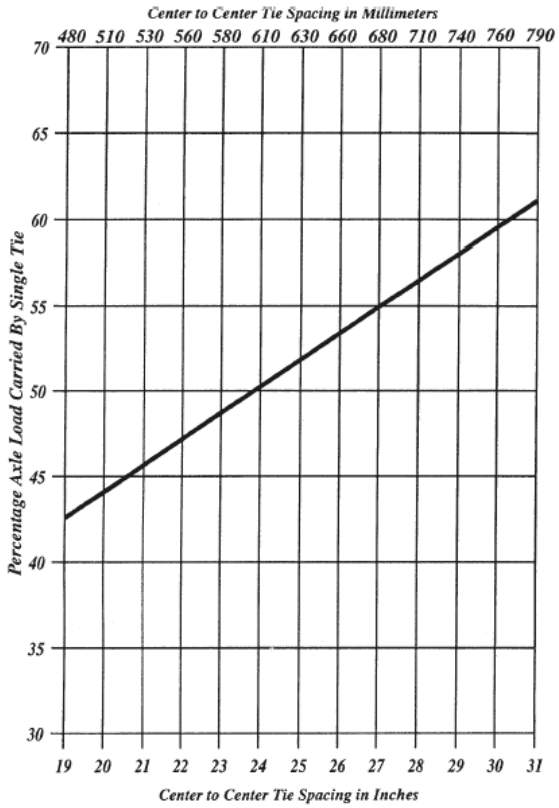

Figure 3-3 Estimated distribution of loads

3.2.4 Finite element modelling of ballast track

The cross section of the track is used in accordance with Ethiopian Railway Corporation (ERC) design standard [22] and the drawing is shown in Figure 3-4. The sectional dimensions and material properties of the track components are detailed in Table 3-5.

Table 3-3 Main technical parameters of national railway line[22]

Scope	**Sebeta~Adama**	**Adama~Djibouti Port**
Track gauge	1435mm	1435mm
No of main lines	Double Track	Single Track
Speed target value	Passenger train: 120km/h Freight train: 80km/h	Passenger train: 120km/h Freight train: 80km/h
Maximum Grade	Ruling grade: 9‰, pusher grade: 18.5‰	Ruling grade: 9‰, pusher grade: 18.5‰
Type of traction	Electric Power	Electric Power
Type of train	Passenger Train：SS9 Freight Train：SS4	Passenger Train：SS9 Freight Train：SS4

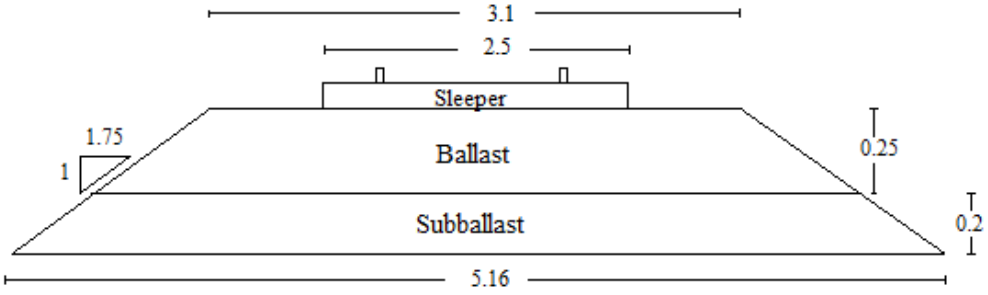

Figure 3-4 Cross-section of the ballast track (units in m)

The geometry of the track is developed by using ANSYS14.5 Design Modeller. The rail, sleepers, ballast and subballast are modelled as three-dimensional elastic solid elements and railpads are modelled as spring-dashpot elements. The total length of the track model is set to be 3m.

Because physical contacting bodies do not interpenetrate, the application must establish a relationship between the two surfaces to prevent them from passing through each other in the analysis. For nonlinear solid body contact of faces, Pure Penalty or Augmented Lagrange formulations can be used. Compared to the Pure Penalty method, Augmented Lagrange formulation usually leads to better conditioning and is less sensitive to the magnitude of the contact stiffness coefficient.[25] Hence for this analysis Augmented Lagrange formulation is used.

Due to the symmetry of the model both in geometry and loading, only half of the model is considered for analysis to decrease the number of elements and reduce analysis time.

The vertical planes of all sides of the model are constrained from displacing laterally and the base of the model is restricted from any displacement.

Since it is practical to improve track property before increasing load above its design limit, two types of track models are generated. The track model in the Figure 3-5 (Model 1) is for the existing track with 50kg/m rail and Railpad 1 and the model in the Figure 3-6 (Model 2) is the track model with improved track property, i.e. with rail 60 kg/m and Railpad 2.

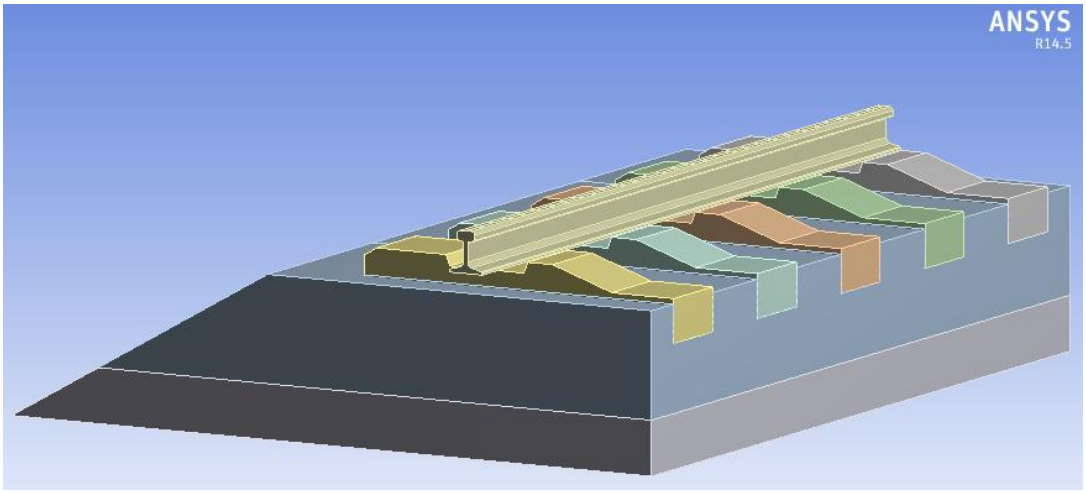

Figure 3-5 Ballast track model across the symmetry with 50kg/m rail and railpad 1 (Model 1)

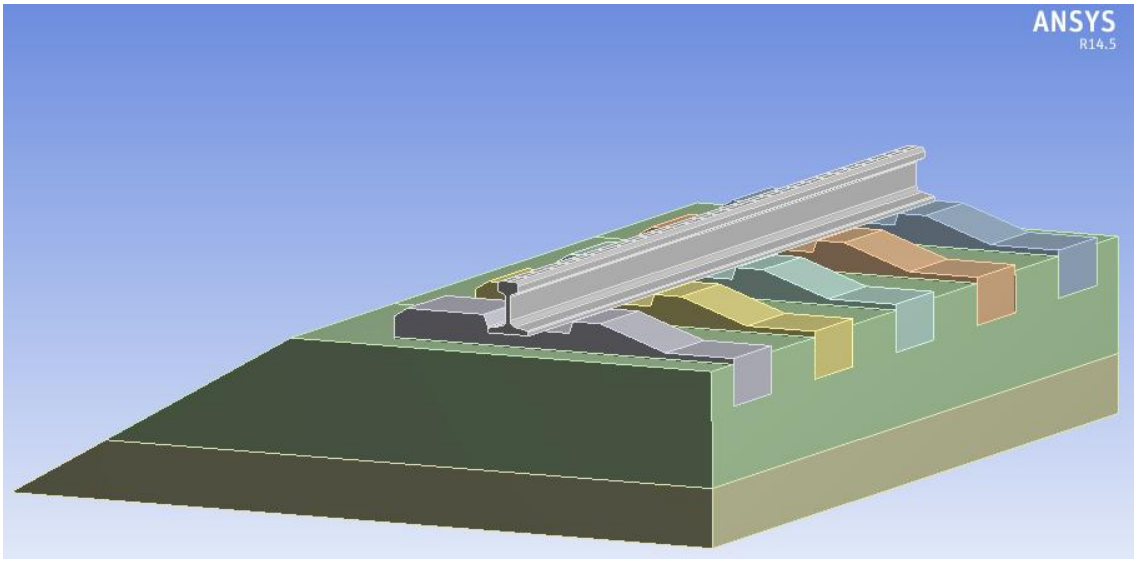

Figure 3-6 Ballast track model across the symmetry with 60 kg/m rail and railpad 2 (Model 2)

Figure 3-7 Spring-dashpot element

Table 3-4 Section property of different rail types

Rail type	**50 kg/m**	**60 kg/m**
Rail height, mm	152	176
Width of rail head, mm	70	73
Web thickness, mm	15.5	16.5
Rail foot width, mm	132	150
Moment of inertia Ixx, cm^4	2037	3217
Moment of inertia Iyy, cm^4	377	524
Section modulus of top, cm^3	251.3	339.4
Section modulus of bottom, cm^3	287.2	369

Table 3-5 Geometrical and mechanical features of the track models

Section	Dimension and Material Property	Remark
Rail	Length = 3000 mm	50kg/m and 60kg/m
	Density = 7829 kg/m^3	
	Young's Modulus = 206 GPa	
	Poisson's Ratio = 0.3	
Railpad 1	Thickness = 10 mm	Spring-dashpot element
	Stiffness = 80kN/mm	
	Damping = 45Ns/mm	
Railpad 2	Thickness = 10 mm	
	Stiffness = 110kN/mm	
	Damping = 63Ns/mm	
Sleeper	Height = 240 mm	600 mm spacing
	Width = 280 mm	
	Length = 2500 mm	
	Density = 2400 kg/m^3	
	Young's Modulus = 36 GPa	
	Poisson's Ratio = 0.2	
Ballast	Thickness = 250 mm	
	Density = 1900 kg/m^3	
	Young's Modulus = 180 MPa	
	Poisson's Ratio = 0.27	
Subballast	Thickness = 200 mm	
	Density = 1900 kg/m^3	
	Young's Modulus = 180 MPa	
	Poisson's Ratio = 0.3	

3.2.5 Finite element modelling of concrete sleeper

Finite element analysis (FEA) provides a tool that can simulate and predict the responses of reinforced and prestressed concrete members. [26]

A three-dimensional geometry of a separate Type II sleeper was generated by ANSYS12 workbench Design Modeller (Figure 3-8) and transferred to Mechanical APDL (ANSYS Parametric Design Language) for modelling and analysis.

The dedicated solid bricks (SOLID65) represent the concrete and the embedded three-dimensional spar elements (LINK8) are used as the prestressing wires. The pre-tensioning was modelled using an initial strain in the tendons corresponding to the prestressing forces at final stage (sustained prestressing force after all losses). [26]

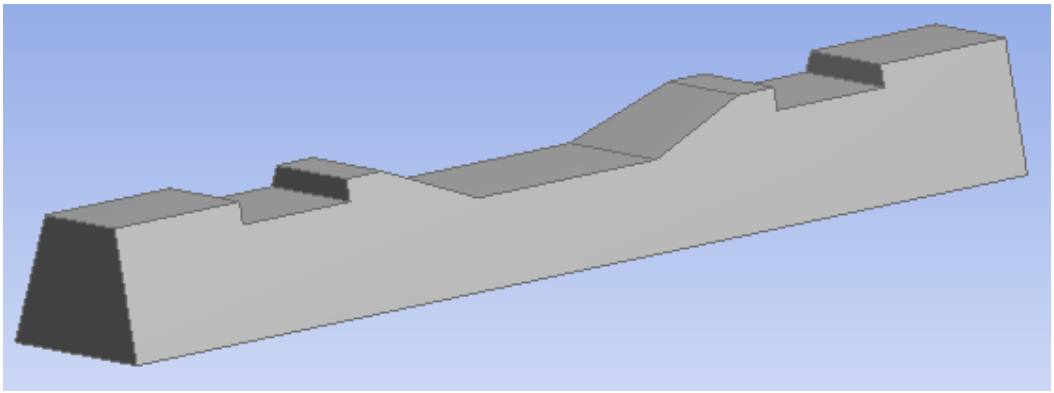

Figure 3-8 Concrete sleeper geometry

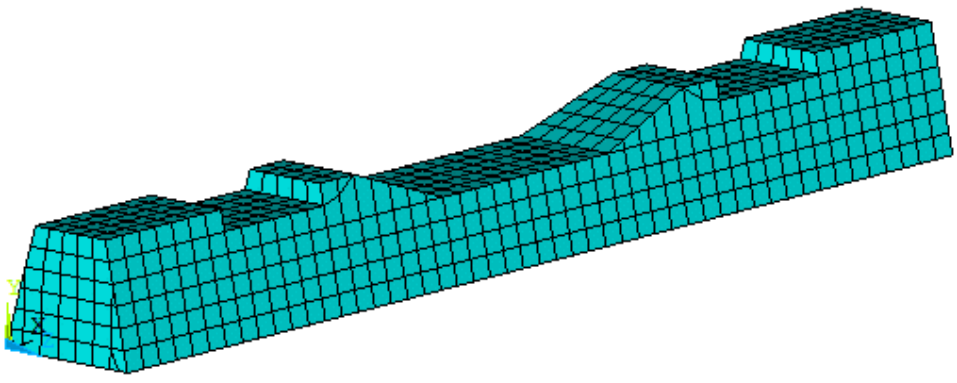

Figure 3-9 Finite element model of concrete sleeper

3.2.5.1 Elements

SOLID65

The concrete part of the sleeper was modelled using a three-dimensional solid element, SOLID65, which has the material model to predict the failure of brittle materials. This element is used for the 3-D modelling of solids with or without reinforcing bars (rebar). The solid is capable of cracking in tension and crushing in compression. In concrete applications, for example, the solid capability of the element may be used to model the concrete while the rebar capability is available for modelling reinforcement behaviour. The element is defined by eight nodes having three degrees of freedom at each node: translations in the nodal x, y, and z directions. Up to three different rebar specifications may be defined.[26][27]

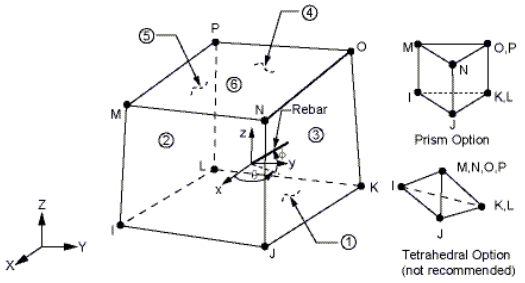

Figure 3-10 SOLID65 geometry[27]

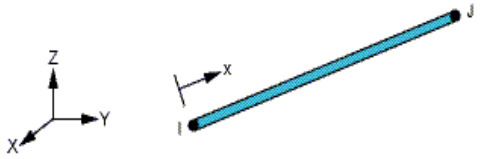

Figure 3-11 LINK8 geometry[27]

LINK8

To simulate the behaviour of prestressing wires, a truss element, LINK8, were used to withstand the initial strain attributed to prestressing forces, by assuming perfect bond between these elements and concrete. This element is a spar which may be used in a variety of engineering applications. It can be used to model trusses, sagging cables, links, springs, etc. The 3-D spar element is a uniaxial tension-compression element with three degrees of freedom at each node: translations in the nodal x, y, and z directions. As in a pin-jointed structure, no bending of the element is considered. Plasticity, creep, swelling, stress stiffening, and large deflection capabilities are included. [26][27]

CHAPTER 4 FINITE ELEMENT ANALYSIS AND RESULTS

In the preceding chapter the three dimensional modelling of ballast track to obtain railseat load is done. Next the separate three dimensional Type II sleeper which is currently being in use for Ethiopian railway lines is modelled in detail. The geometry, material property, elements used, etc which are parameters used in the modelling are mentioned in the preceding chapter.

In this section the analysis results of both the models (ballast track and Type II sleeper models) are presented. The railseat load is obtained from the dynamic analysis of ballast track models (Model 1 and Model 2) and the ballast support pressure is calculated by applying two types of support conditions (as mentioned in section 3.2.3.2). Finally the Type II prestressed concrete sleeper model is statically analysed to obtain the bending stress and deflection in the cases of increasing train speed and axle load by considering the above mentioned types of support conditions.

The effect of increase in speed and axle load under variable ballast support condition along the length of the sleeper and the effect of improving track property on the structural response of the concrete sleeper at both rail seat and centre section of the sleeper are discussed.

4.1 Dynamic Analysis of the Track Model

The dynamic effects of moving loads on the track system can be divided into two groups: on the one hand, the dynamic effects due to the variation of amount and direction of the forces induced by the wheels; on the other hand, the effects due to their movement with more or less high speed. [28]

Loading

Train load is modelled as the sequence of discrete pulses loads at the rail nodes. Therefore, the spacing of the loading nodes are divided by the train speed results to time step of calculation, and the software automatically applies it to the analysis model as a dynamic nodal. The dynamic load on the sleeper is obtained in the form of reaction time histories at the rail-seat locations. [29][30]

Design wheel load is defined as the product of static wheel load and a corrective factor known as dynamic impact factor to compensate for dynamic as well as impact effects of wheel load resulted from wheel and rail surface irregularities.[31]

In this track model analysis a transient load is applied on the rail nodes for dynamic analysis and to consider wheel and rail surface irregularity effect, the impact factor formula developed by AREMA is used.

$$P = ØP_s \quad (4.1)$$

where P = design wheel load (kN),

P_s= static wheel load (kN) and

Ø = dimensionless impact factor (always >l).

$$Ø = 1 + 5.21\frac{V}{D} \quad (4.2)$$

where V = vehicle speed (km/h), and

D = wheel diameter (mm)

For speed 80 km/h and axle load 21 ton the design wheel load will be

$$P_s = \frac{21\ ton*1000kg*10m/s^2}{2} = 105 \text{ kN}$$

$$Ø = 1 + 5.21*\frac{80}{1200} = 1.347$$

$$P = 1.347*105 \text{ kN} = 141.47 \text{ kN}$$

The time history of rail seat load is obtained from track model analysis and shown in the figures, Figure 4-2 and Figure 4-3 for speed and Figure 4-4 and Figure 4-5 for axle load.

4.1.1 Speed

The maximum speed of passenger trains on the national railway lines is suggested to be set at 120 km/h.[22] To study the effect of increase in speed, the speed at rates of 80, 120, 160 and 200 km/h are considered and axle load 21 ton (SS9 locomotive) is used.

Table 4-1 Design wheel load for increasing speed

Speed (km/h)	Impact factor	Design wheel load (kN)
80	1.347	141.47
120	1.521	159.71
160	1.695	177.94
200	1.868	196.18

The diagram of the wheel load against the time for speed of 80 km/h and axle load 21 ton is shown in the Figure 4-1 as an example.

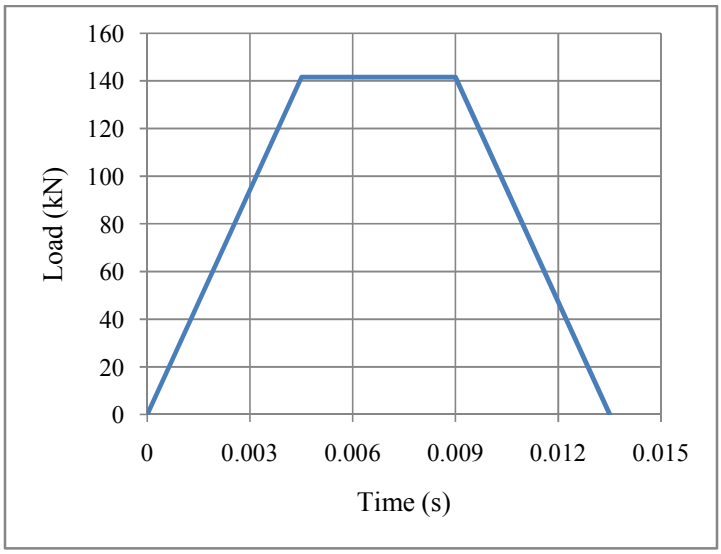

Figure 4-1 Time step diagram for 80 km/h speed

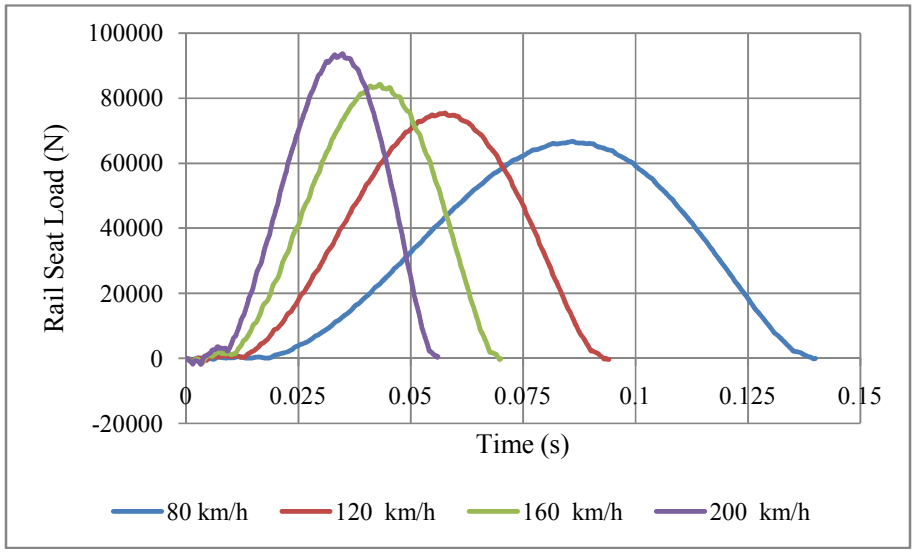

Figure 4-2 Time history of rail seat load due to increasing speed with Model 1

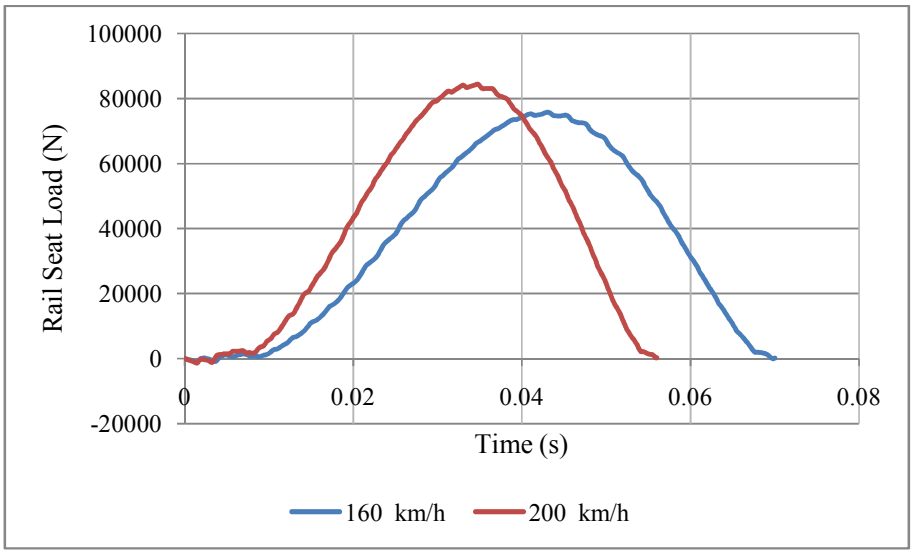

Figure 4-3 Time history of rail seat load due to increasing speed with Model 2

Table 4-2 Railseat load for increase in speed

Speed (km/h)	Railseat Load (N)	
	Model 1	Model 2
80	66701	
120	75383	
160	84203	75754
200	93609	84369

4.1.2 Axle load

Railways around the world with similar rail and sleeper specifications have axle load limits ranging from 22.5 to 32.5tons/axle.[11]

According to [22] speed for freight trains is to be set at 80km/h and the axle load is 23ton (SS4 locomotive). Since the higher axle loads are common with freight trains to study the effect of increase in axle load on the sleeper the design speed for freight trains which is 80 km/h is used and incremental rates of axle load at 23, 25, 27 and 29 tons are considered.

Table 4-3 Design wheel load for increasing axle load

Axle Load (ton)	Impact factor	Design wheel load (kN)
23	1.347	154.94
25	1.347	168.42
27	1.347	181.89
29	1.347	195.36

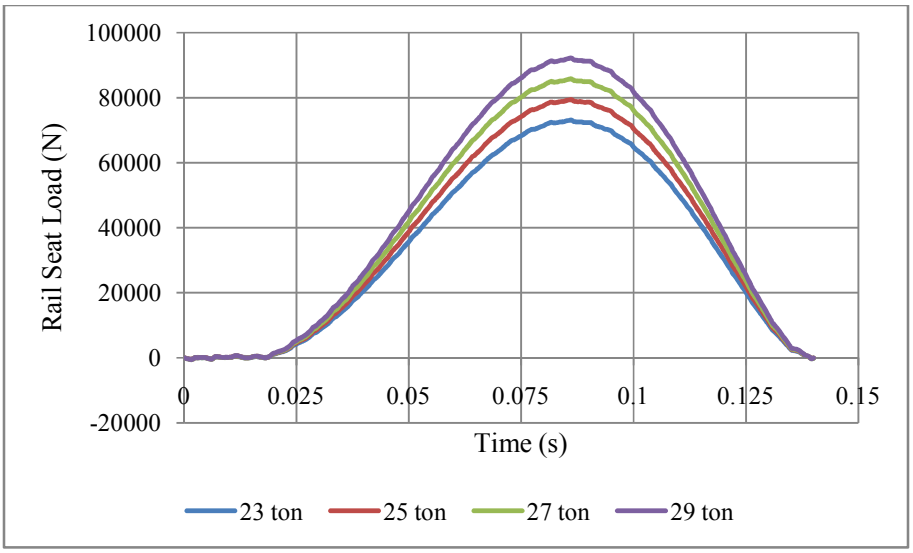

Figure 4-4 Time history of rail seat load due to increasing axle load with Model 1

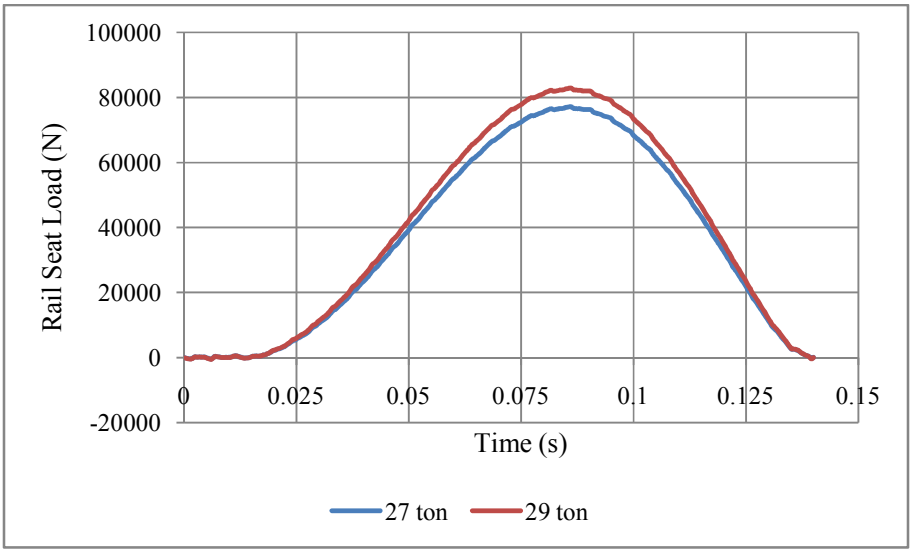

Figure 4-5 Time history of rail seat load due to increasing axle load with Model 2

Table 4-4 Railseat load for increasing value of axle load

Axle Load (ton)	Railseat Load (N)	
	Model 1	Model 2
23	73061	
25	79428	
27	85783	77212
29	92144	82949

4.1.3 Ballast pressure

The rail seat load is obtained from sections 4.1.1 and 4.1.2.

Bearing area of the sleeper = 280 * 2500 = 700,000 mm^2

Case 1 ($L_{eff} \cong 2L/3$)

Ballast Pressure (MPa) = $\frac{3q}{A} <$ 65psi (0.448MPa)

where, q = Rail seat load (N)

A = bearing area (mm^2)

Table 4-5 Ballast pressure for case 1 support condition

Speed (km/h)	Ballast Pressure (MPa)	
	Model 1	Model 2
80	0.2859	
120	0.3231	
160	0.3609	0.3247
200	0.4012	0.3616
Axle Load (ton)		
23	0.3131	
25	0.3404	
27	0.3676	0.3309
29	0.3949	0.3555

Case 2 (L_{eff} = L)

Ballast Pressure (MPa) = $\frac{2q}{A}$ < 85psi (0.586MPa)

where, q = Rail seat load (N)

A = bearing area (mm^2)

Table 4-6 Ballast pressure for case 2 support condition

Speed (km/h)	Ballast Pressure (MPa)	
	Model 1	Model 2
80	0.1906	
120	0.2154	
160	0.2406	0.2164
200	0.2675	0.2411
Axle Load (ton)		
23	0.2087	
25	0.2269	
27	0.2451	0.2206
29	0.2633	0.2370

4.2 Static Analysis of the Sleeper Model

The static structural analysis is employed in ANSYS12 to study the response (bending stress and deflection) of the prestressed concrete sleeper to varying speed and axle load under the two types of ballast support conditions. In this analysis the ballast pressure is used to simulate loading on the sleeper. The analysis is done in four different conditions as it is shown in the sections 4.2.1, 4.2.2, 4.2.3 and 4.2.4 with results.

These are:-

i. Increase in speed under Case 1($L_{eff} \cong 2L/3$) support condition

ii. Increase in speed under Case 2(L_{eff} = L) support condition

iii. Increase in axle load under Case 1($L_{eff} \cong 2L/3$) support condition

iv. Increase in axle load under Case 2 (L_{eff} = L) support condition

4.2.1 Increase in speed under Case 1($L_{eff} \cong 2L/3$) support condition

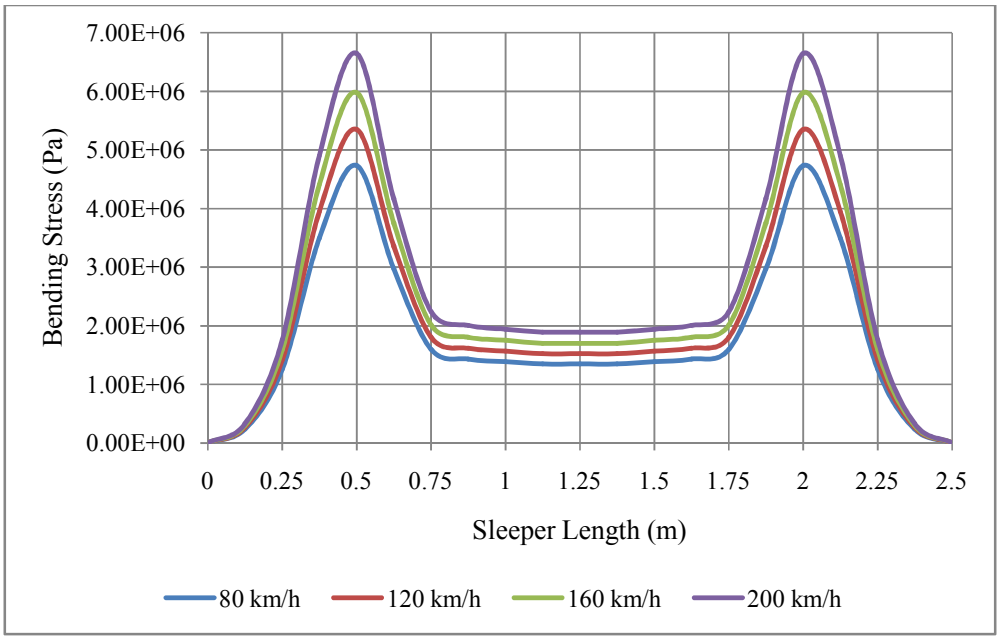

Figure 4-6 Bending stress diagram for speed under Case 1 support condition (Model 1)

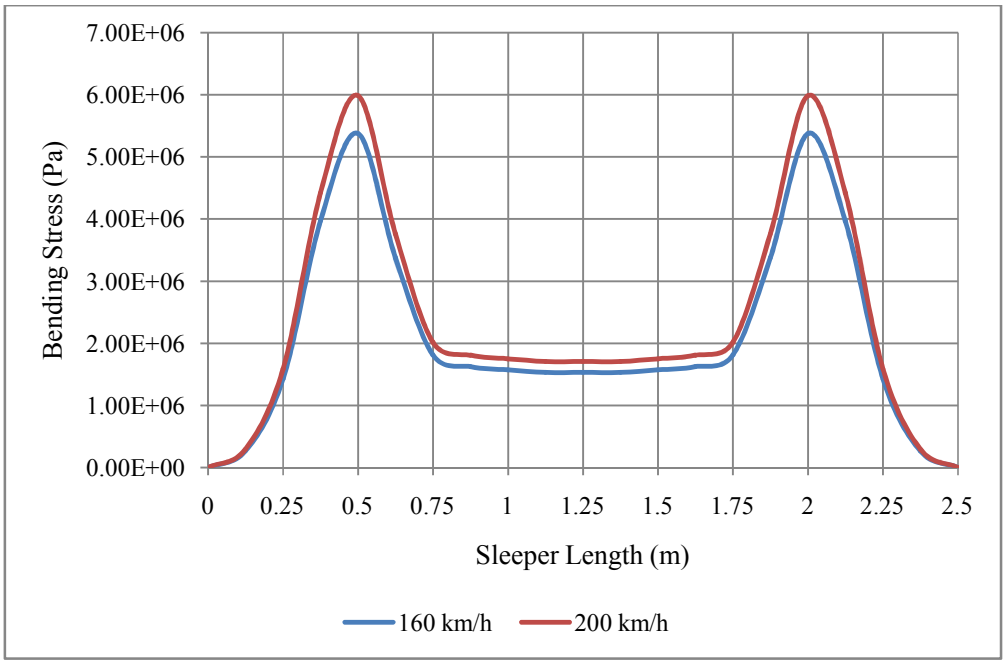

Figure 4-7 Bending stress diagram for speed under Case 1 support condition (Model 2)

Table 4-7 Maximum Bending stress for speed under Case 1 support

Speed (km/h)	Bending Stress (Pa)			
	Model 1		Model 2	
	Rail seat	Centre	Rail seat	Centre
80	4.73E+06	1.35E+06		
120	5.35E+06	1.52E+06		
160	5.98E+06	1.70E+06	5.38E+06	1.53E+06
200	6.64E+06	1.89E+06	5.99E+06	1.70E+06

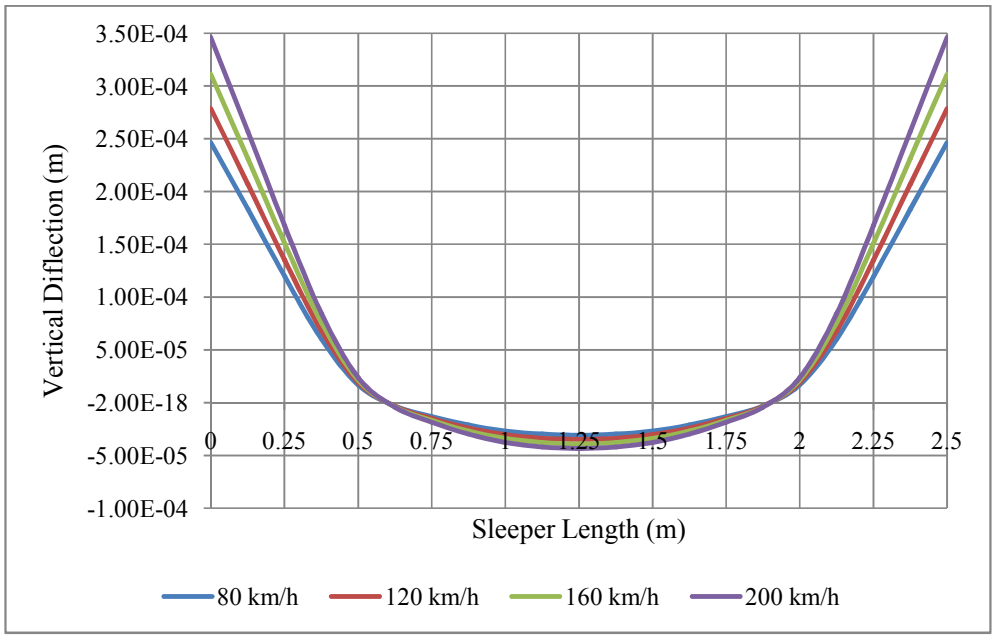

Figure 4-8 Vertical deflection diagram for speed under Case 1 support condition (Model 1)

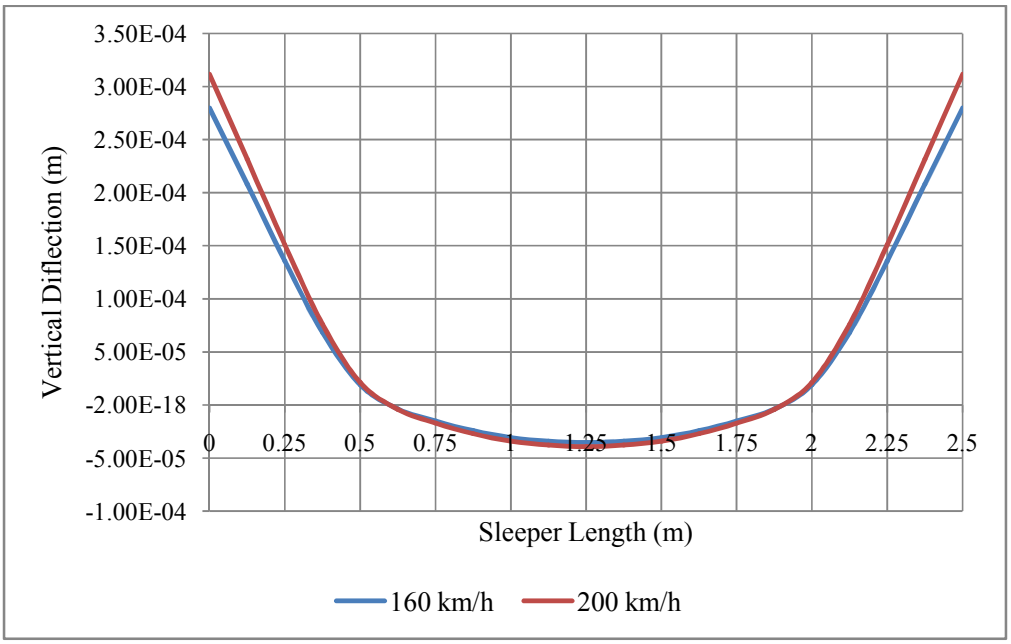

Figure 4-9 Vertical deflection diagram for speed under Case 1 support condition (Model 2)

Table 4-8 Maximum vertical deflection for speed under Case 1 support

Speed (km/h)	Vertical Deflection (m)			
	Model 1		Model 2	
	Rail seat	Centre	Rail seat	Centre
80	1.68E-05	-3.10E-05		
120	1.89E-05	-3.50E-05		
160	2.12E-05	-3.91E-05	1.90E-05	-3.52E-05
200	2.35E-05	-4.35E-05	2.12E-05	-3.92E-05

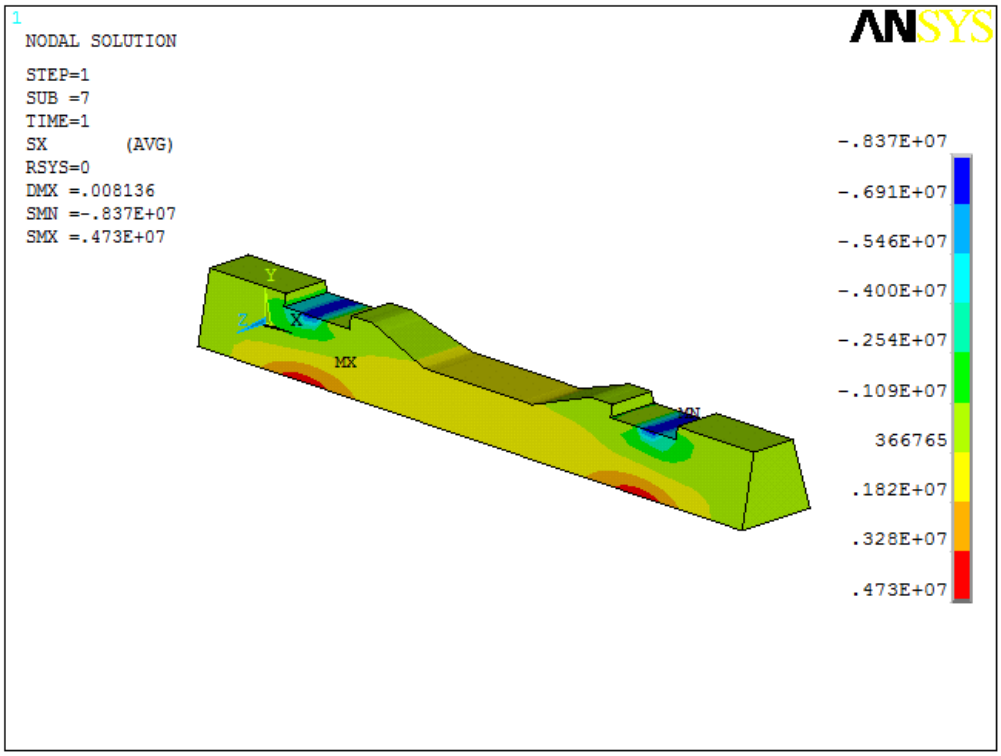

Figure 4-10 Contour plot of bending stress for speed (80 km/h) under Case 1 support

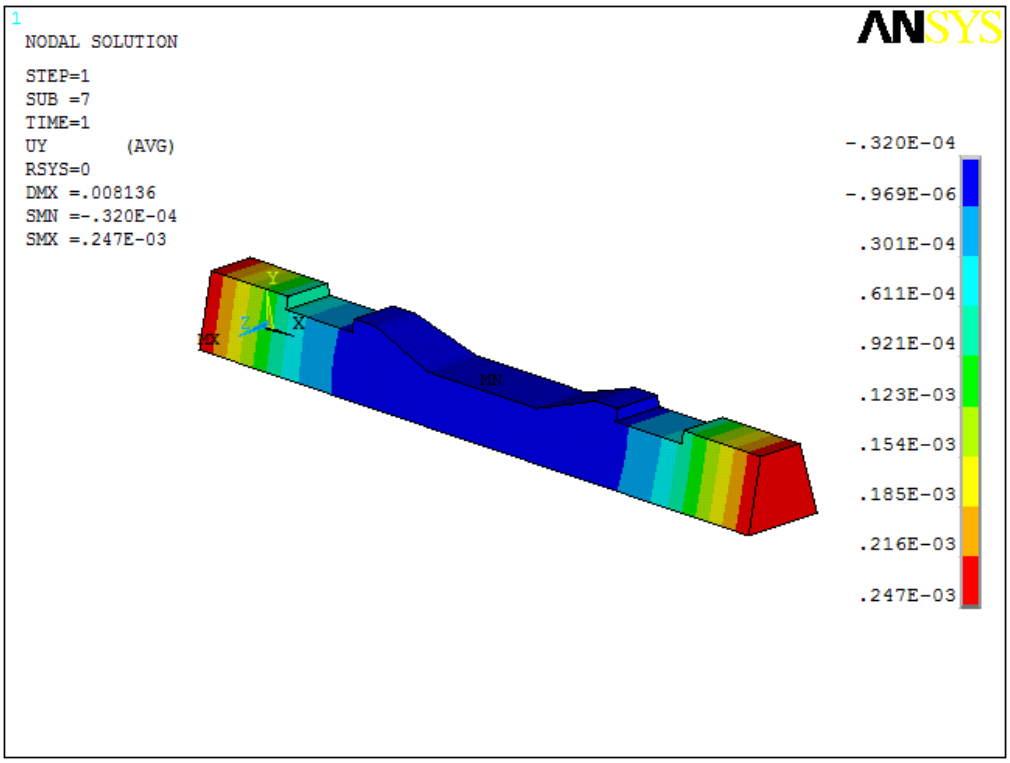

Figure 4-11 Contour plot of vertical deflection for speed (80 km/h) under Case 1 support

4.2.2 Increase in speed under Case 2 (L_{eff} = L) support condition

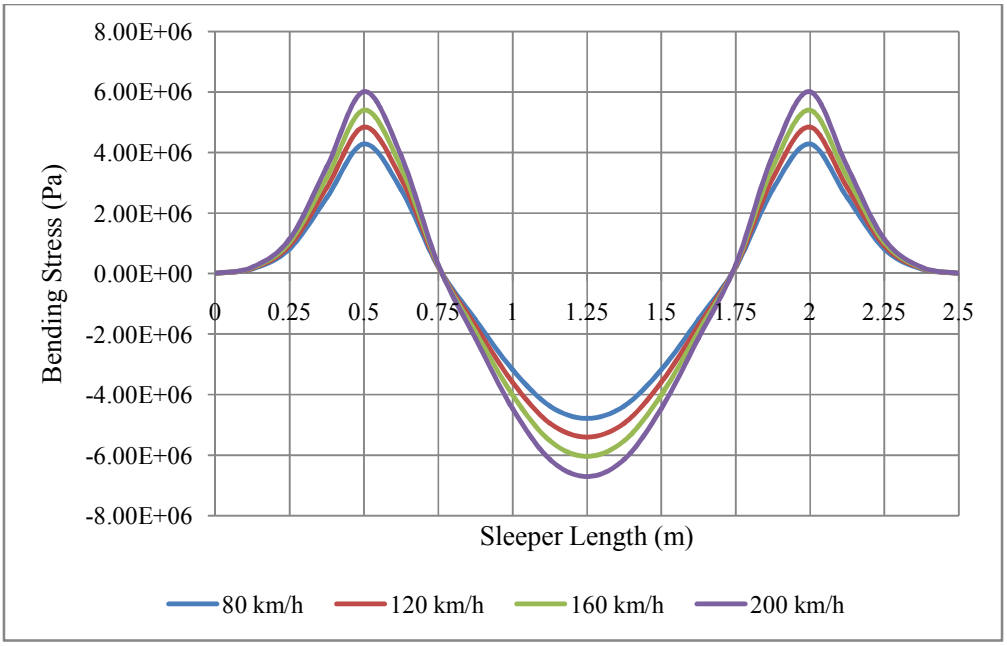

Figure 4-12 Bending stress diagram for speed under Case 2 support condition (Model 1)

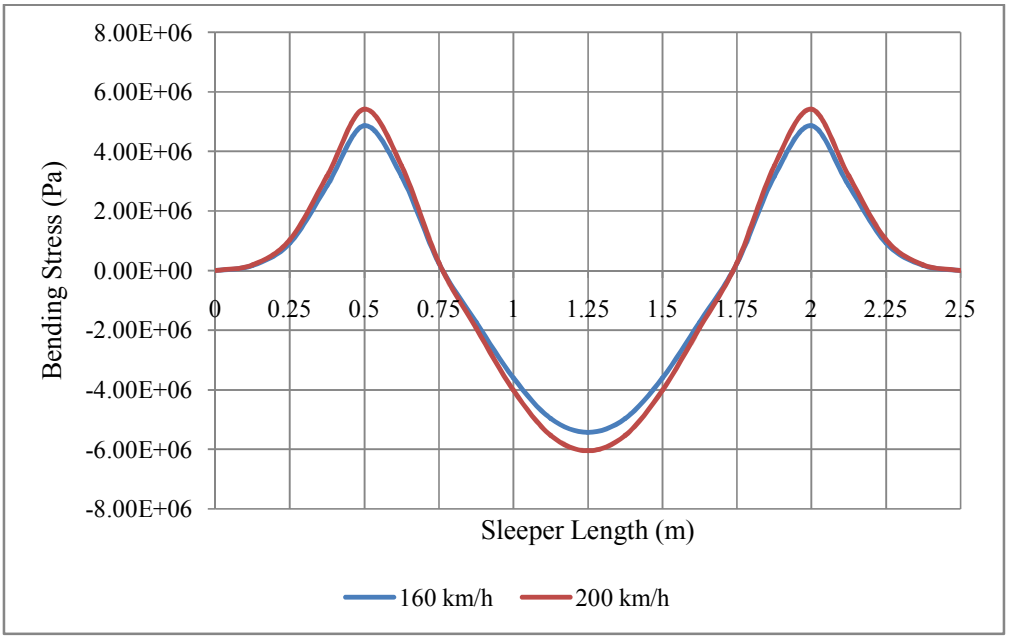

Figure 4-13 Bending stress diagram for speed under Case 2 support condition (Model 2)

Table 4-9 Maximum Bending stress for speed under Case 2 support

Speed (km/h)	Bending Stress (Pa)			
	Model 1		Model 2	
	Rail seat	Centre	Rail seat	Centre
80	4.28E+06	-4.78E+06		
120	4.84E+06	-5.40E+06		
160	5.40E+06	-6.04E+06	4.86E+06	-5.43E+06
200	6.01E+06	-6.71E+06	5.41E+06	-6.05E+06

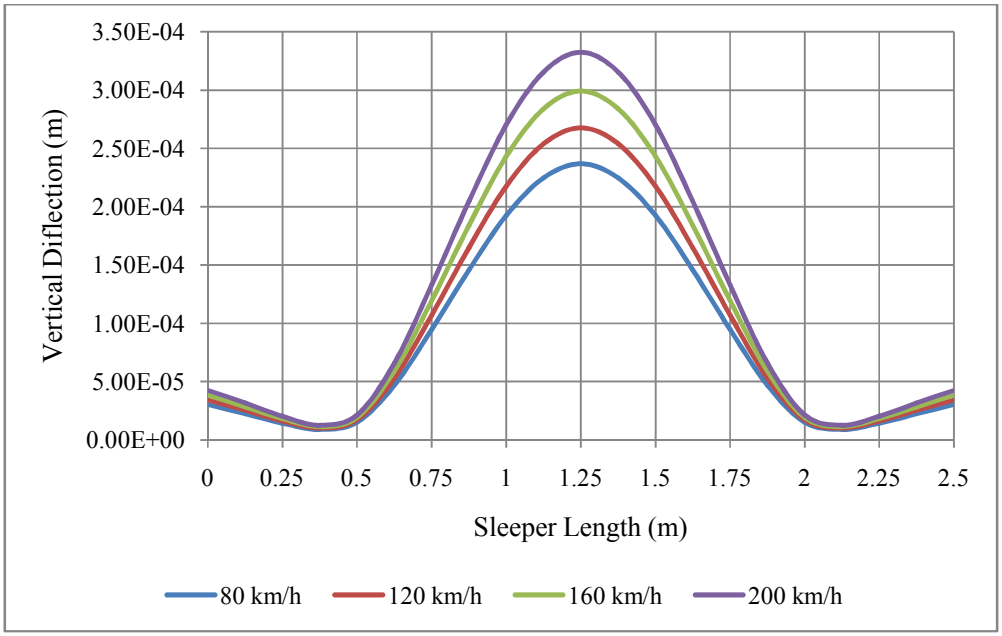

Figure 4-14 Vertical deflection diagram for speed under Case 2 support condition (Model 1)

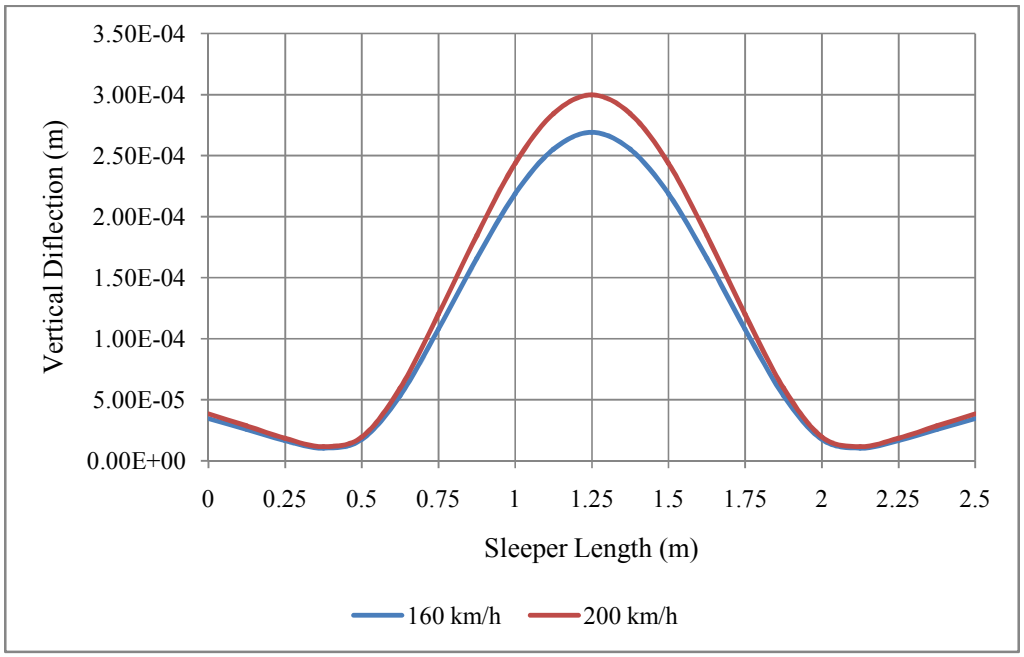

Figure 4-15 Vertical deflection diagram for speed under Case 2 support condition (Model 2)

Table 4-10 Maximum vertical deflection for speed under Case 2 support

Speed (km/h)	Vertical Deflection (m)			
	Model 1		Model 2	
	Rail seat	Centre	Rail seat	Centre
80	1.53E-05	2.37E-04		
120	1.73E-05	2.68E-04		
160	1.94E-05	2.99E-04	1.74E-05	2.69E-04
200	2.15E-05	3.32E-04	1.94E-05	3.00E-04

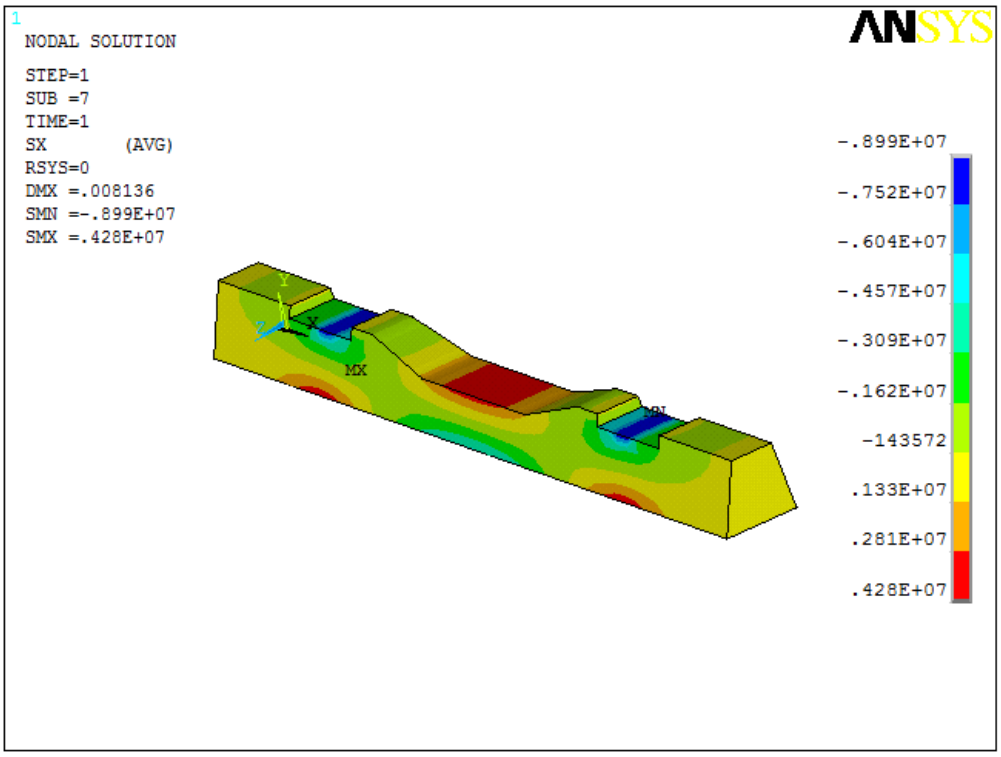

Figure 4-16 Contour plot of bending stress for speed (80 km/h) under Case 2 support

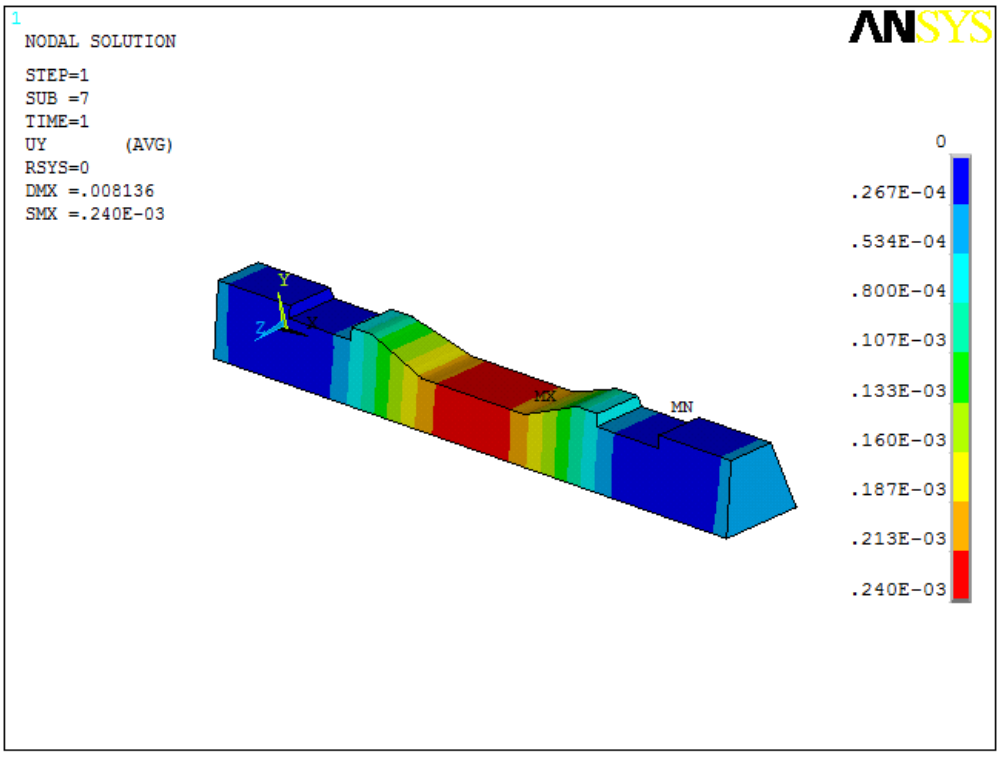

Figure 4-17 Contour plot of vertical deflection for speed (80 km/h) under Case 2 support

4.2.3 Increase in axle load under Case 1 ($L_{eff} \cong 2L/3$) support condition

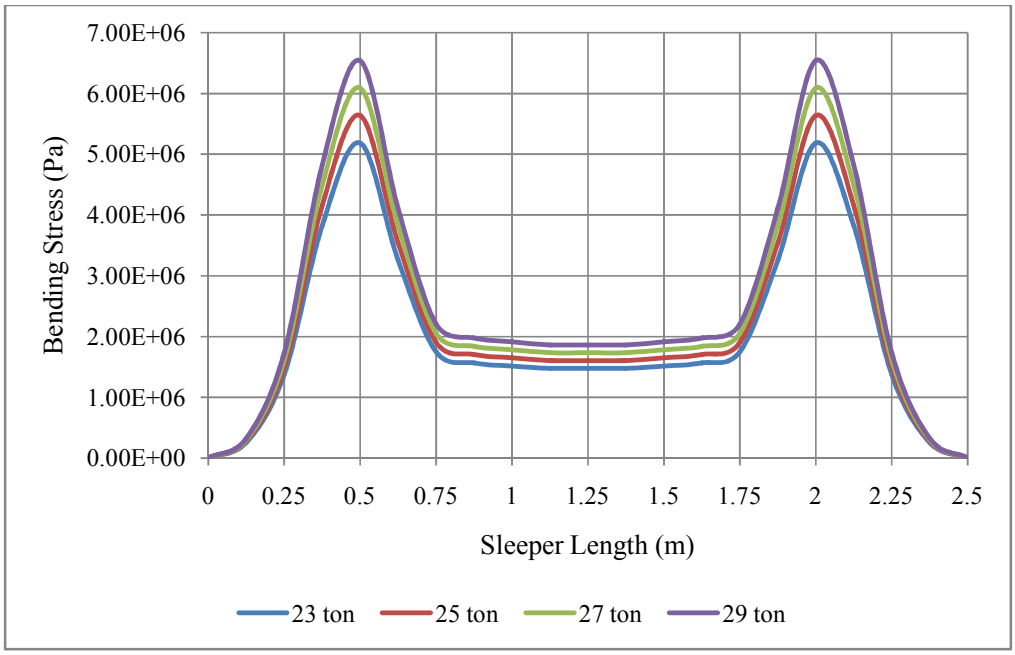

Figure 4-18 Bending stress diagram for axle load under Case 1 support condition (Model 1)

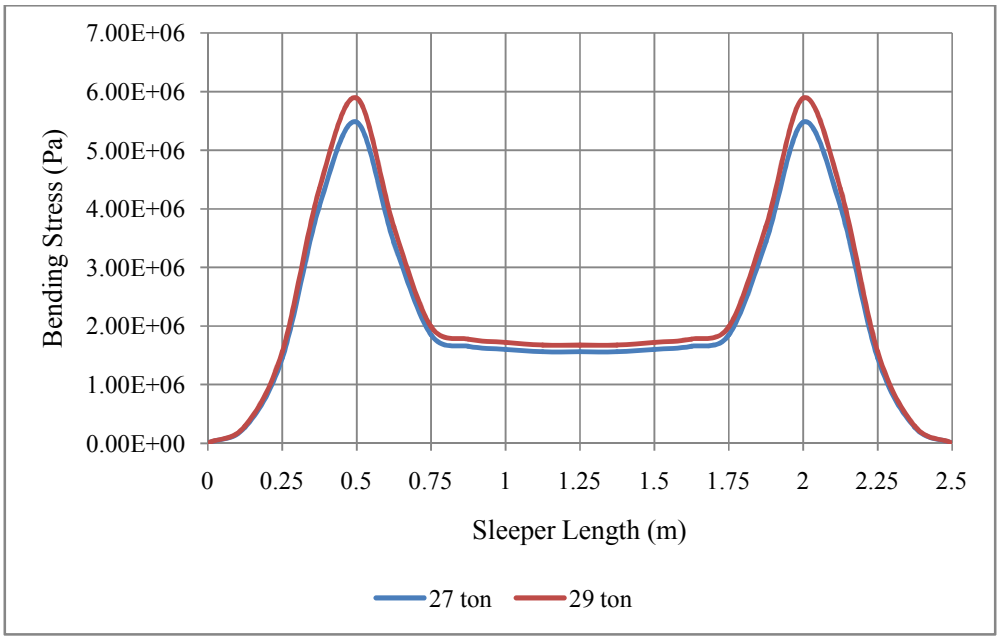

Figure 4-19 Bending stress diagram for axle load under Case 1 support condition (Model 2)

Table 4-11 Maximum Bending stress for axle load under Case 1 support

Axle Load (ton)	Bending Stress (Pa)			
	Model 1		Model 2	
	Rail seat	Centre	Rail seat	Centre
23	5.18E+06	1.48E+06		
25	5.64E+06	1.60E+06		
27	6.09E+06	1.73E+06	5.48E+06	1.56E+06
29	6.54E+06	1.86E+06	5.89E+06	1.68E+06

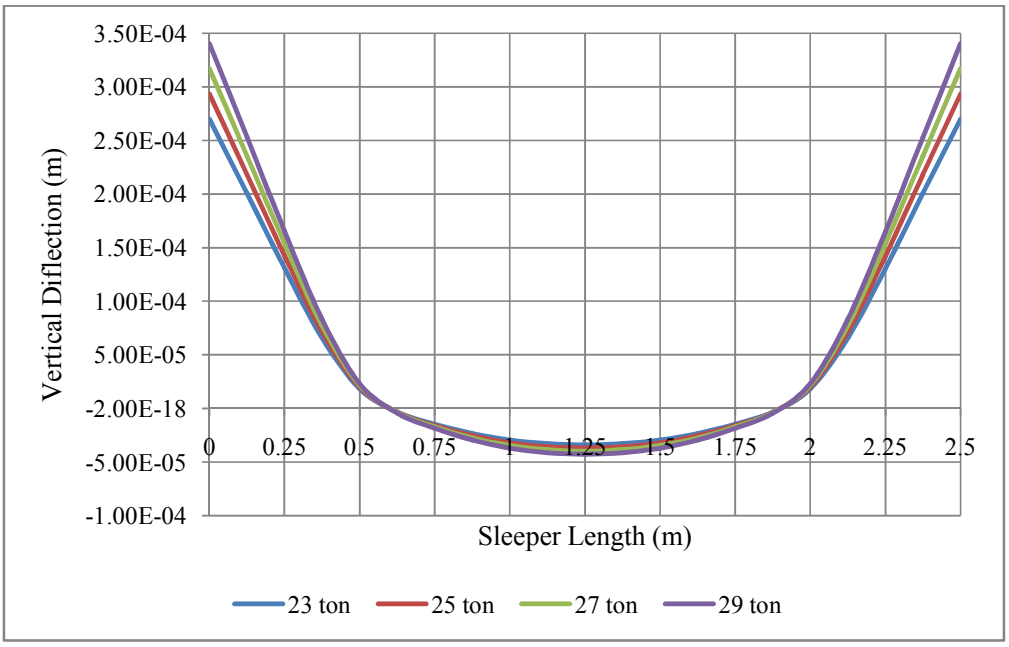

Figure 4-20 Vertical deflection diagram for axle load under Case 1 support condition (Model 1)

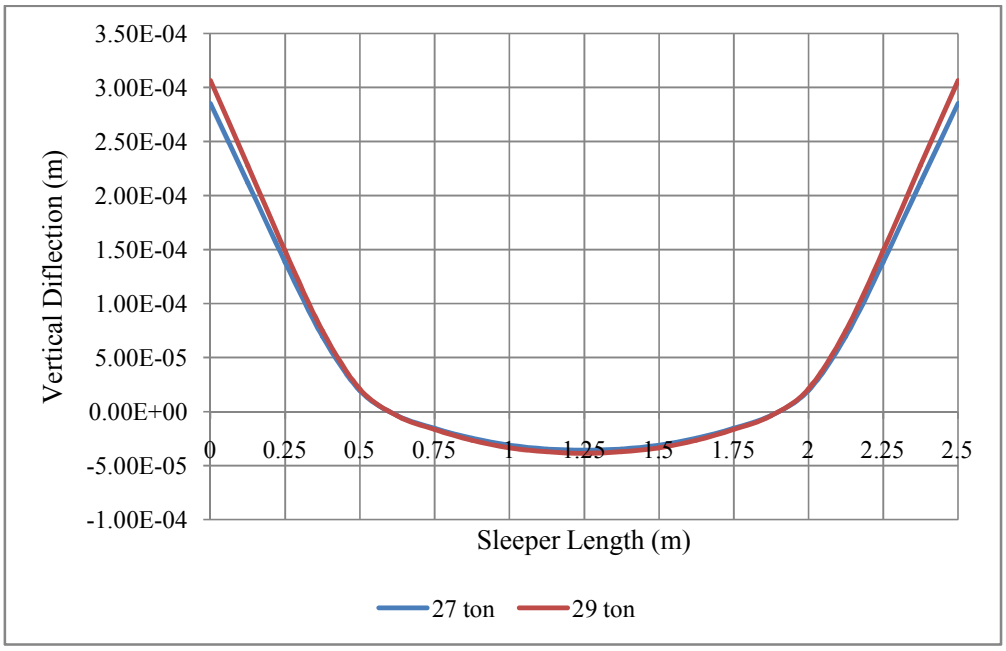

Figure 4-21 Vertical deflection diagram for axle load under Case 1 support condition (Model 2)

Table 4-12 Maximum vertical deflection for axle load under Case 1 support

Axle Load (ton)	Vertical Deflection (m)			
	Model 1		Model 2	
	Rail seat	Centre	Rail seat	Centre
23	1.84E-05	-3.40E-05		
25	2.00E-05	-3.69E-05		
27	2.16E-05	-3.99E-05	1.94E-05	-3.59E-05
29	2.31E-05	-4.28E-05	2.08E-05	-3.86E-05

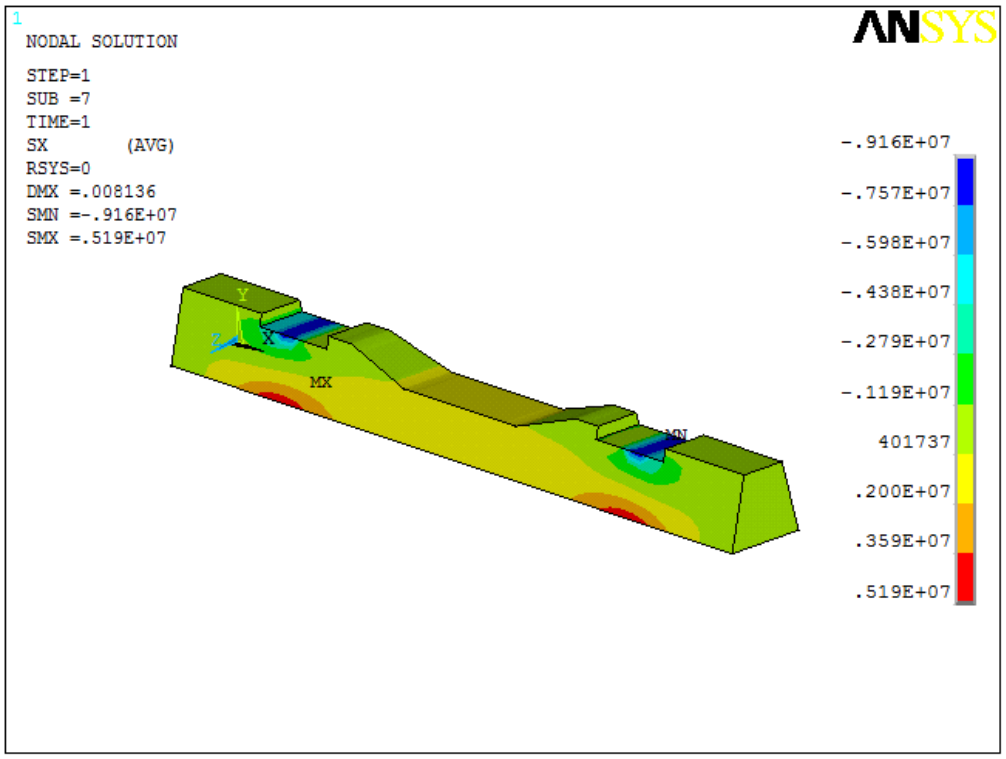

Figure 4-22 Contour plot of bending stress for axle load (23 ton) under Case 1 support

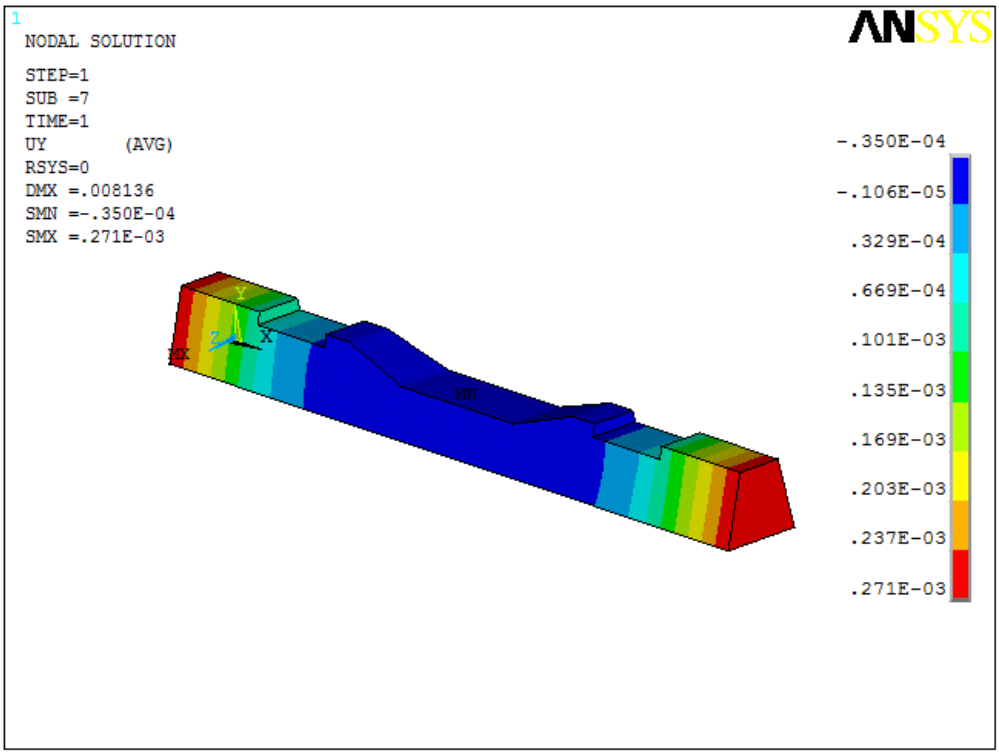

Figure 4-23 Contour plot of vertical deflection for axle load (23 ton) under Case 1 support

4.2.4 Increase in axle load under Case 2 (L_{eff} = L) support condition

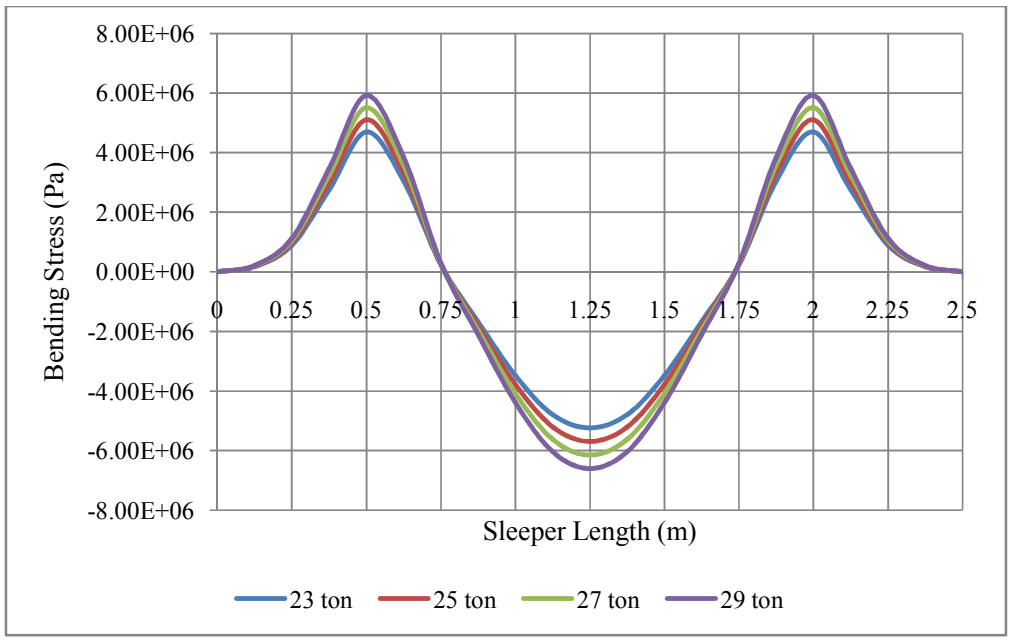

Figure 4-24 Bending stress diagram for axle load under Case 2 support condition (Model 1)

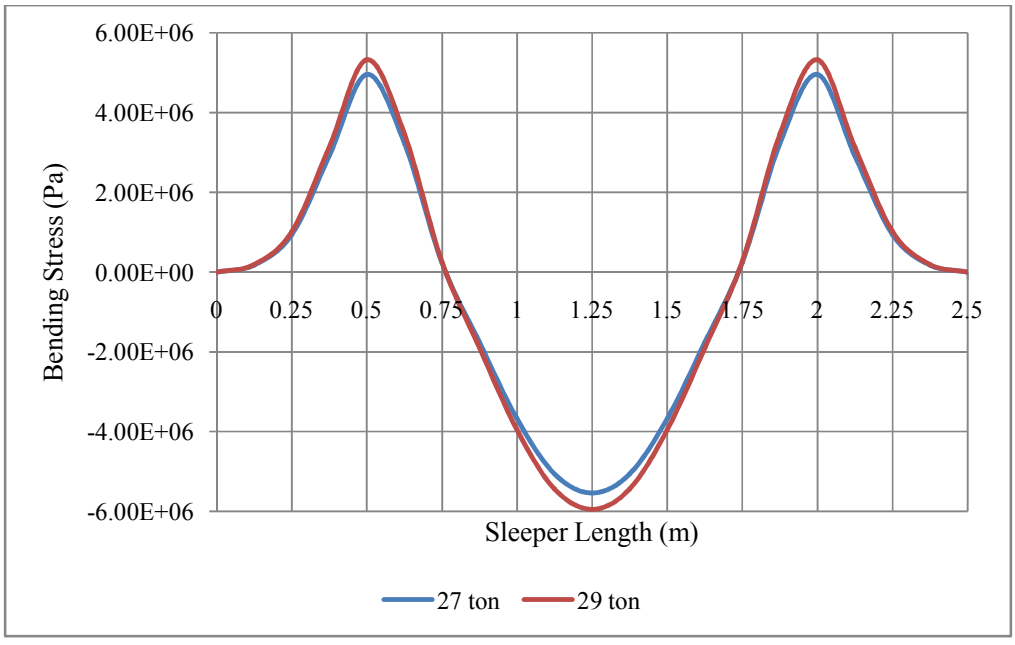

Figure 4-25 Bending stress diagram for axle load under Case 2 support condition (Model 2)

Table 4-13 Maximum Bending stress for axle load under Case 2 support

Axle Load (ton)	Bending Stress (Pa)			
	Model 1		Model 2	
	Rail seat	Centre	Rail seat	Centre
23	4.69E+06	-5.24E+06		
25	5.10E+06	-5.69E+06		
27	5.51E+06	-6.15E+06	4.96E+06	-5.53E+06
29	5.91E+06	-6.60E+06	5.32E+06	-5.95E+06

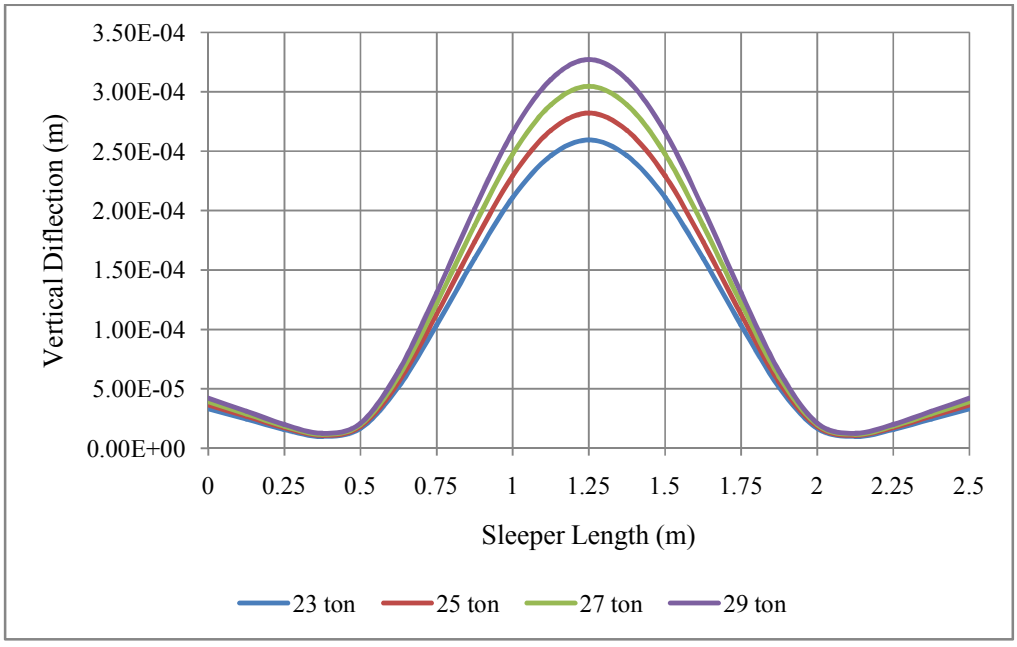

Figure 4-26 Vertical deflection diagram for axle load under Case 2 support condition (Model 1)

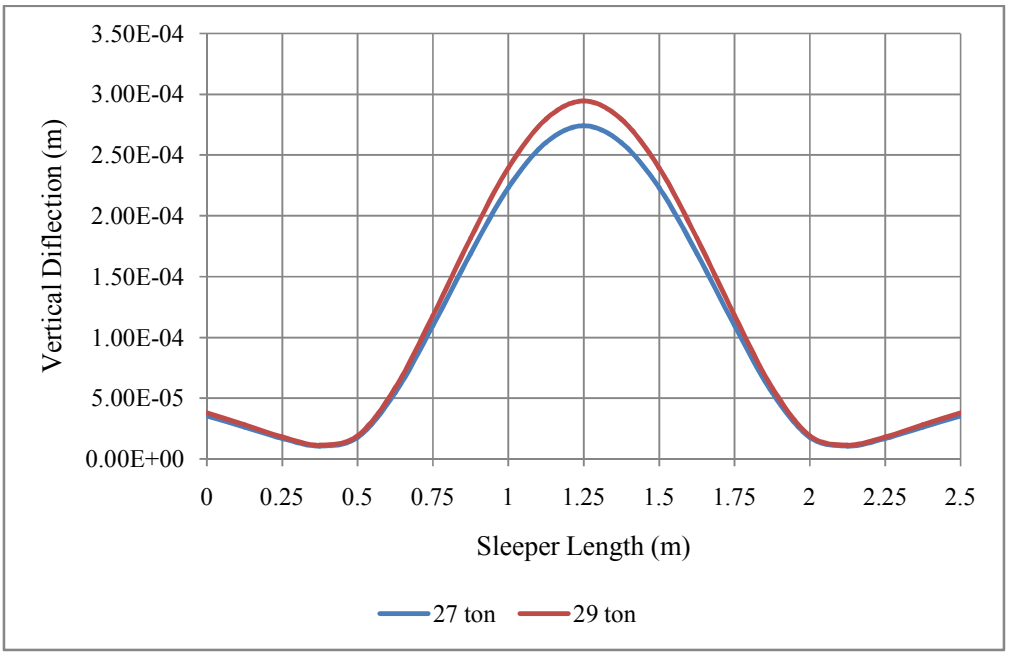

Figure 4-27 Vertical deflection diagram for axle load under Case 2 support condition (Model 2)

Table 4-14 Maximum vertical deflection for axle load under Case 2 support

Axle Load (ton)	Vertical Deflection (m)			
	Model 1		Model 2	
	Rail seat	Centre	Rail seat	Centre
23	1.68E-05	2.59E-04		
25	1.83E-05	2.82E-04		
27	1.97E-05	3.05E-04	1.78E-05	2.74E-04
29	2.12E-05	3.27E-04	1.91E-05	2.94E-04

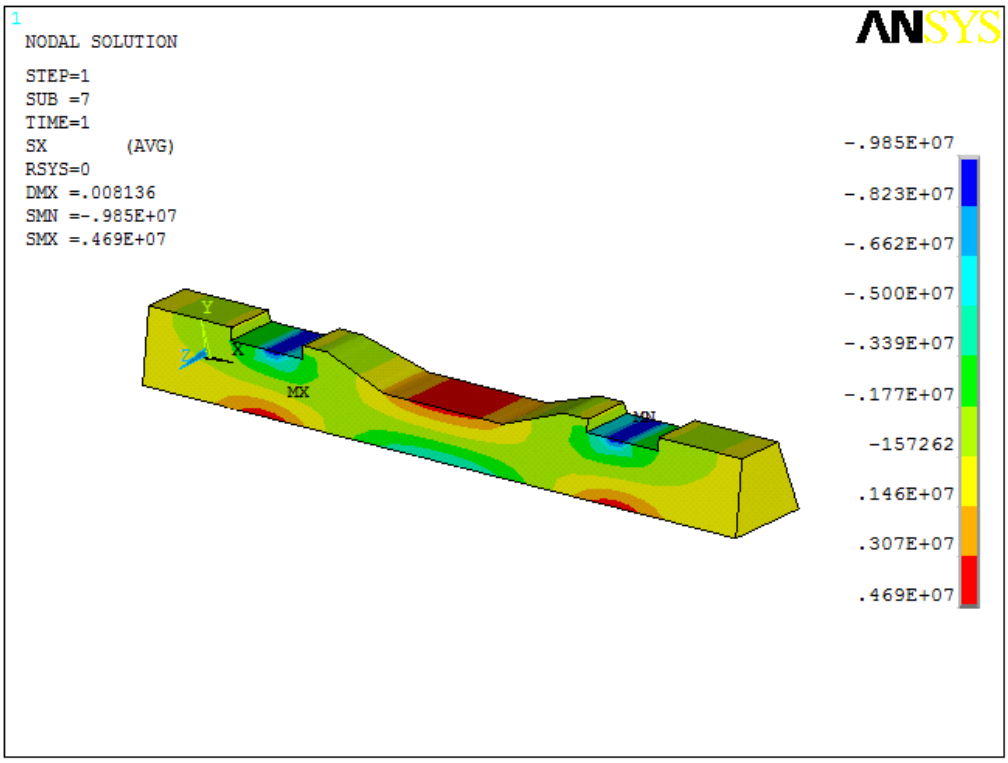

Figure 4-28 Contour plot of bending stress for axle load (23 ton) under Case 2 support

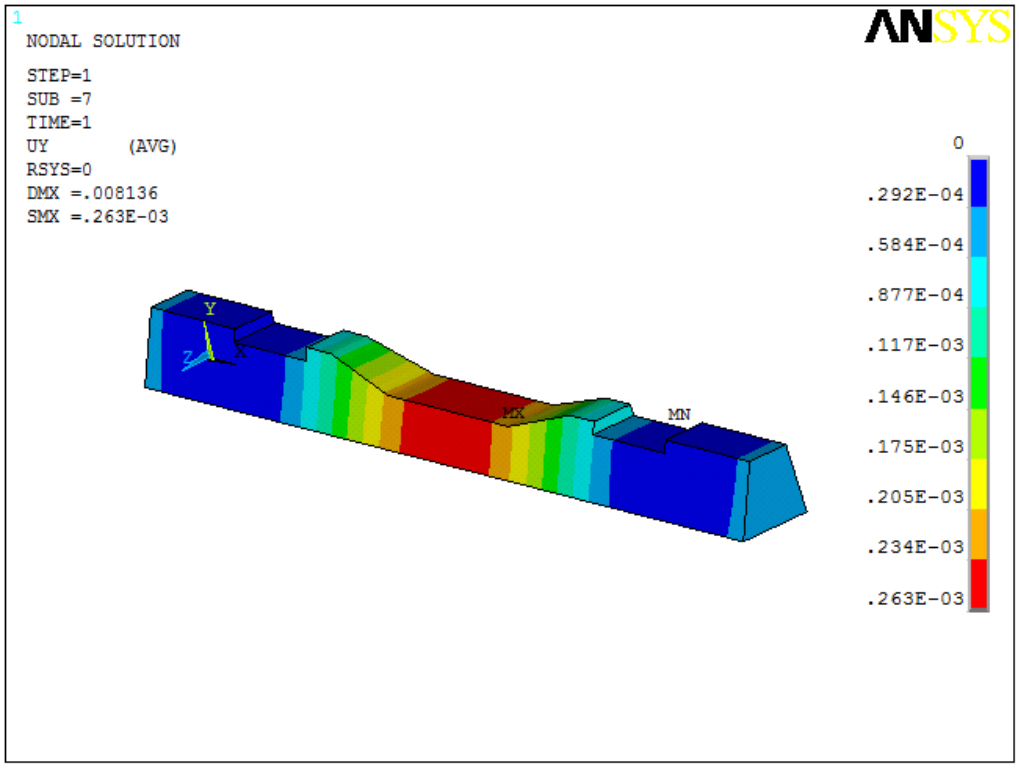

Figure 4-29 Contour plot of vertical deflection for axle load (23 ton) under Case 2 support

4.3 Discussion

Rail seat load

The results from the simulation of 3-D ballast track models show that in the case of increasing train speed and axle load the amount of wheel load transferred to the sleeper is incremental.

To investigate the sensitivity of rail seat load to speed, the unfactored rail seat load (i.e. rail seat load divided by impact factor) from the track Model 1 is considered. As it can be seen in the Figure 4.30, the railseat load increment is low up to the speed limit of about 160 km/h and there is a very significant increase when the speed exceeds this value. From this figure the relationship between speed and rail seat load can be obtained as

$$y = 0.0006x^3 - 0.1846x^2 + 20.8709x + 48724 \qquad (4.3)$$

in which x represents speed in km/h and y represents rail seat load in N.

In the case of increase in axle load Figure 4.31 shows that the relationship between rail seat load and axle load is linear. This relationship can be obtained from the figure as

$$y = 2360.366x - 60 \qquad (4.4)$$

where x is axle load in ton and y is rail seat load in N.

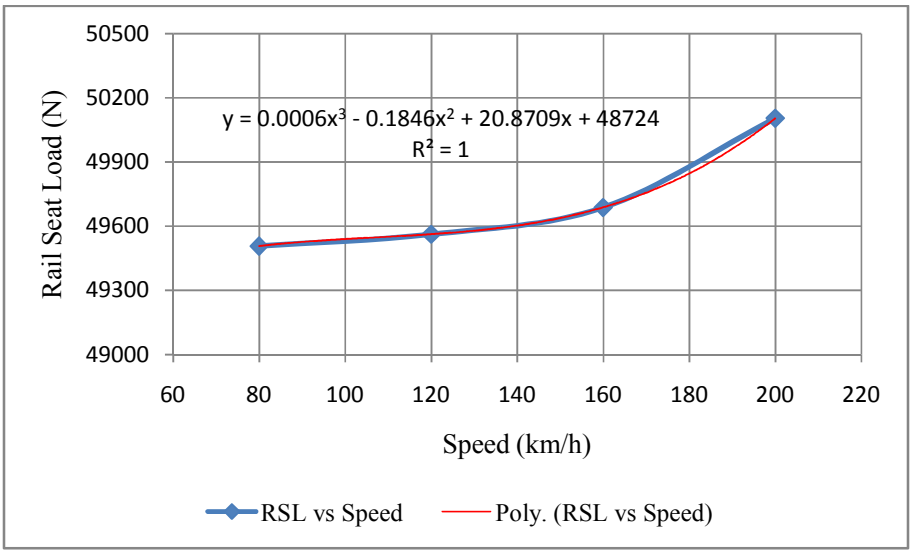

Figure 4-30 Rail seat load versus train speed

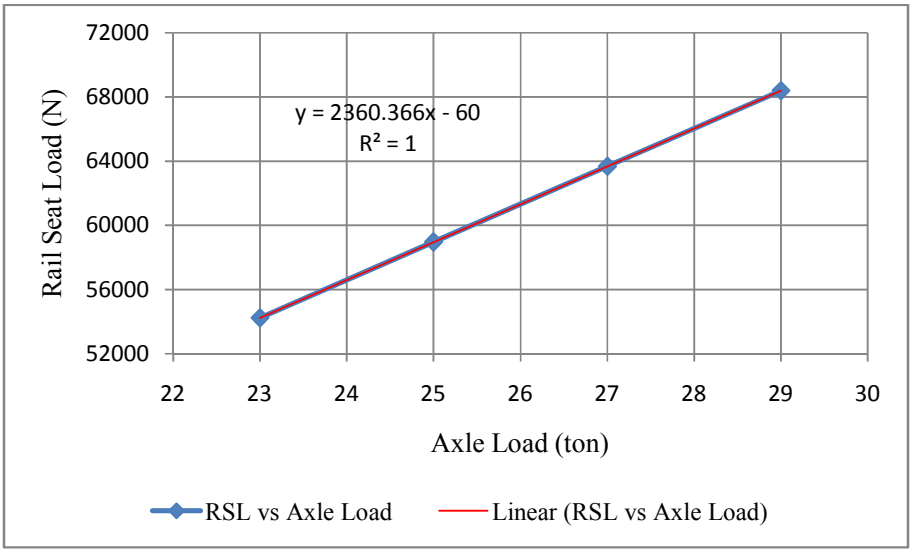

Figure 4-31 Rail seat load versus axle load

Bending stress

As it can be seen in the charts (Figure 4-6, 4-7, 4-18, 4-19) for increasing speed and axle load under Case 1 ($L_{eff} \cong 2L/3$) type of ballast support condition, the bending stress is positive both at rail seat and centre sections. The maximum positive occurs at the railseat and minimum positive around the centre sections along the sleeper length. This means, the sleeper under Case 1 support condition is subjected to tensile stress at both sections of the sleeper with higher tension at the railseat and lower at the centre sections. This tensile stress increases with increasing speed and axle load for both the sections.

Charts (Figure 4-12, 4-13, 4-24, 4-25) show that for increasing speed and axle load under Case 2 ($L_{eff} = L$) ballast support condition, the bending stress is maximum positive at railseat and negative at the centre along the length of the sleeper. This means that the railseat section is subjected to the highest tensile stress and the centre section is subjected to the highest compressive stress along the length of the sleeper. Also it has been shown that under increasing speed and axle load, both railseat and centre sections are becoming subjected to higher tensile and compressive stresses respectively.

In the case of speed the percentage increment of bending stress is about 13% when it increases from 80 km/h to 120 km/h and it gets to 11.7% when the speed increment is from 120 km/h to 160 km/h and 11.2% (11.4% with Model 2) when the speed increases from 160 km/h to 200 km/h.

In the case of increasing axle load the percentage increment of bending stress is linear. It is 8.7% when the axle load increases from 23 ton to 25 ton and it gets to 8% when the axle load changes from 25 ton to 27 ton and 7.4% (similar with Model 2) when the axle load increases from 27 ton to 29 ton.

Generally, the percentage increment of bending stress in the case of speed is about 40.3% when the speed rate changes from 80 km/h to 200 km/h (150% increment) and in the case of axle load the percentage increment is about 26.1% when the axle load increases from 23 ton to 29 ton (26.1% increment) at both rail seat and centre sections with track Model 1.

With the same increment in speed and axle load, the improved track model (Model 2) reduced the percentage increment of bending stress by about 13.8% (40.3% to 26.5%) in the case of speed and about 12.6% (26.1% to 13.5%) in the case of axle load.

Deflection

In the charts (Figure 4-8, 4-9, 4-20, 4-21) for increasing speed and axle load the vertical deflection is positive at rail seat (maximum at the corner) and negative at the centre of the sleeper. This implies the vertical deflection is upward around the rail seat and downward around the centre section along the length of the sleeper under Case 1 support condition.

In figures (Figure 4-14, 4-15, 4-26, 4-27) the vertical deflection is positive throughout the length of the sleeper. This deflection attains its highest at the centre and lowest at the railseat sections. This shows that the vertical deflection is upward throughout the length of the sleeper and maximum upward deflection occurs at the centre and minimum at the railseat sections of the sleeper under Case 2 support condition. These deflections also increase with the increase in speed and axle load.

Similar to that of bending stress with the same increment in speed and axle load, improved track model (Model 2) reduced the percentage increment of deflection by about 13.8% in the case of speed and about 12.6% in the case of axle load.

CHAPTER 5 CONCLUSIONS AND RECCOMENDATIONS

5.1 Conclusion

The objective of this thesis is to study the effect of increase in speed and axle load on the structural response of prestressed concrete sleeper under two kinds of ballast support conditions which are mentioned in AREMA manual. These two kinds of supports are categorised as Case 1($L_{eff} \cong 2L/3$) and Case 2 ($L_{eff} = L$) for the purpose of this thesis. Since it is practical to improve track property before increasing load above its design limit, the existing track model (Model 1) is modified to obtain a track model with a better rail profile and pad stiffness (Model 2) and the effect of track improvement on the structural response of sleeper under increased train speed and axle load is investigated.

To do this a three-dimensional ballast track and a separate concrete sleeper with a detailed feature are modelled and analysed by using commercial finite element package, ANSYS. Both dynamic and static types of structural analysis are employed to get railseat load in the case of dynamic analysis and to find bending stress and deflection of the sleeper in the case of static analysis.

The analysis results show that increasing the train speed and axle load affects the structural behaviour of the sleeper by increasing the bending stress and deflection.

The increase in speed from 80 to 200 km/h which is 150% increment increases the bending stress and deflection of the sleeper in about 40.3% and increase in axle load from 23 ton to 29 ton which is 26.1% increment increases the bending stress and deflection in about 26.1% with both types of the ballast support conditions and track Model 1.

With the same increment in speed and axle load, improving the track model (Model 2) reduced the percentage increment of bending stress and deflection by about 13.8% in the case of speed and 12.6% in the case of axle load.

As it has been seen in the previous chapter, the numerical results exhibit that the bending stress and deflection of the sleeper are affected slightly by the speed variation of the train and they are affected significantly by the increment of axle load.

It is also shown that the condition of ballast support underneath the sleeper plays a great role on the structural response of the sleeper.

5.2 Recommendation and Further Research

As it can be clearly seen in the discussion section, the effect of increase in both speed and axle load increases the bending stress and deflection of the sleeper. But when the comparison is between the two, it shows that the effect of increase in axle load is much higher than that of the speed. When it comes to the comparison between the support conditions within the effect of speed and axle load, it is also seen that for the same increment in speed and axle load under the two types of ballast support conditions, Case 1 shows the higher tensile bending stress at railseat section of the sleeper than Case 2 type of support condition and Case 2 shows the higher compressive bending stress at sleeper centre than Case 1 type of ballast support. Therefore, it should be of concern for sleeper designers, manufacturers, track contractors, etc. to consider the condition of ballast support such as distribution of the ballast underneath the sleeper before increasing speed and axle load and much care should be taken while increasing axle load than speed.

In this study the effect of increase in speed and axle load on sleeper structural response is considered separately which means that to study the speed effect axle load is remained constant and vice versa, hence further research can be done to investigate the combined effect of both conditions. In addition, the train model is only simulated as point loading in this thesis. More forward steps can be done to simulate the train model in ANSYS. Also, the results should be compared with field tests in order to obtain final verification.

Sleepers in turnout are subjected to loadings and support condition considerably different from sleepers in tangent track. The passage of train generate a non-uniform dynamic load and understanding how the turnout sleepers respond to the exerted dynamic forces is important and worth a study. Hence, for the further research the effect of speed and axle load on the structural response of turnout sleepers can be considered.

REFERENCES

1. Ernest T. Selig and John M. Waters, 1994. *Track Geotechnology and Substructure Management*
2. Konstantinos Tzanakakis, 2013. *The Railway Track and Its Long Term Behaviour-A Handbook for a Railway Track of High Quality*
3. Buddhima I., Wadud S. and Cholachat R., 2011. *Advanced Rail Geotechnology-Ballasted Track*
4. Tore Dahlberg, 2006. *Handbook of Railway Vehicle Dynamics- Track Issues*
5. N.F. Doyle, 1980. *Railway Track Design: A Review of Current Practice*
6. Coenraad Esveld, 2001. *Modern Railway Track 2nd Ed.*
7. Tore Dahlberg, 2004. *Railway Track Settlements – A Literature Review*, Report for the EU project SUPERTRACK
8. Ferreira L. and Murray M.,1997. *Modelling Rail Track Deterioration and Maintenance: Current Practices and Future Needs.* Transport Reviews, 17 (3), 207-221
9. Yin Gao, 2013. A 3D Dynamic Train-Track Interaction Model to Study Track Performance under Trains Running at Critical Speed, Master of Science Thesis
10. Huan Feng, 2011. *3D-Models of Railway Track for Dynamic Analysis*, Master Degree Project, Royal Institute of Technology, Stockholm
11. The World Bank, 2011. *Railway Reform: Toolkit for improving Rail Sector Performance*
12. R.I.Gilbert & N.C.Mickleborough, 1990. *Design of Prestressed Concrete*
13. Edward G. Nawy, 2010. *Prestressed Concrete - A Fundamental Approach 5th Ed*.
14. Amlan K. Sengupta and Devdas Menon, Prestressed concrete structures, Indian Institute of Technology Madras, online version
15. N Krishna Raju, 2007. *Prestressed Concrete 4th Ed.*
16. Satish Chandra and M.M. Agarwal, 2007. *Railway Engineering*
17. V.A. Profillidis, 2006. *Railway Management and Engineering 3rd Ed.*
18. Russell H. Lutch, Devin K. Harris and Theresa M. Ahlborn, 2009. *Prestressed Concrete Ties In North America,* AREMA

19. J. M. Sadeghi and M. Youldashkhan, March 2005. *Investigation on the Accuracy of the Current Practices in Analysis of Railway Track Concrete Sleepers,* International Journal of Civil Engineering.
20. Amir N. Hanna, 1979. *State of the Art Report on Prestressed Concrete Ties for North American Railroads*, PCI Journal, Portland Cement Association
21. G. R. Liu and S. S. Quek, 2003. *The Finite Element Method: A Practical Course*
22. Ethiopian Railways Corporation, 2012. *Ethiopia/Sebeta-Djibouti/Nagad Railway Feasibility Study*, Part I General Specification, Executive Edition
23. National Standard of the People's Republic of China, 2002. *Code for Design of Concrete Structures, GB50010-2002*
24. AREMA, 2010. *Manual for Railway Engineering*
25. ANSYS14.5, *Help Manual*
26. S. Kaewunruen and Alexander Remennikov, 2007. *Experimental and Numerical Studies of Railway Prestressed Concrete Sleepers under Static and Impact Loads*, Research Online, University of Wollongong
27. ANSYS12, *Help Manual*
28. Dietmar Adam, Heinz Brandl and Ivan Paulmichl, 2010. *Dynamic Aspects of Rail Tracks for High-Speed Railways*, International Journal of Pavement Engineering
29. Mojtaba Shahraki and Karl Josef Witt, 2015. *3D Modelling of Transition Zone between Ballasted and Ballastless High-Speed Railway Track,* Journal of Traffic and Transportation Engineering
30. G. Kumaran, Devdas Menon and K. Krishnan Nair, 2002. *Evaluation of Dynamic Load on Railtrack Sleepers Based on Vehicle-Track Modelling and Analysis,* International Journal of Structural Stability and Dynamics
31. J. Sadeghi and P. Barati, 2010. *Evaluation of Conventional Methods in Analysis and Design of Railway Track System*, International Journal of Civil Engineering